THE JOURNAL OF COMPARATIVE NEUROLOGY 287:98-118 (1989)

Visual Area MT in the *Cebus* Monkey: Location, Visuotopic Organization, and Variability

MARIO FIORANI, JR., RICARDO GATTASS, MARCELLO G.P. ROSA, AND AGLAI P.B. SOUSA
Instituto de Biofísica Carlos Chagas Filho, Universidade Federal do Rio de Janeiro, Rio de Janeiro, RJ 21941, Brasil

ABSTRACT

The representation of the visual field in the dorsal portion of the superior temporal sulcus (ST) was studied by multiunit recordings in eight *Cebus apella*, anesthetized with N_2O and immobilized with pancuronium bromide, in repeated recording sessions. On the basis of visuotopic organization, myeloarchitecture, and receptive field size, area MT was distinguished from its neighboring areas.

MT is an oval area of about 70 mm^2 located mainly in the posterior bank of the superior temporal sulcus. It contains a visuotopically organized representation of at least the binocular visual field. The representation of the vertical meridian forms the dorsolateral, lateral, and ventrolateral borders of MT and that of the horizontal meridian runs across the posterior bank of ST. The fovea is represented at the lateralmost portion of MT, while the retinal periphery is represented medially.

The representation of the central visual field is magnified relative to that of the periphery in MT. The cortical magnification factor in MT decreases with increasing eccentricity following a negative power function. Receptive field size increases with increasing eccentricity. A method to evaluate the scatter of receptive field position in multiunit recordings based on the inverse of the magnification factor is described. In MT, multiunit receptive field scatter increases with increasing eccentricity.

As shown by the Heidenhain-Woelcke method, MT is coextensive with two myeloarchitectonically distinct zones: one heavily myelinated, located in the posterior bank of ST, and another, less myelinated, located at the junction of the posterior bank with the anterior bank of ST.

At least three additional visual zones surround MT: DZ, MST, and FST. The areas of the dorsal portion of the superior temporal sulcus in the diurnal New World monkey *Cebus* are comparable to those described for the diurnal Old World monkey, *Macaca*. This observation suggests that these areas are ancestral characters of the simian lineage and that the differences observed in the owl monkey may be secondary adaptations to a nocturnal ecological niche.

Key words: prestriate cortex, visual topography, cortical magnification factor, scatter, myeloarchitecture

The organization of the extrastriate visual areas in the Old World monkey *Macaca* differs from that described for the New World monkey *Aotus* (Gattass et al., '86b). These monkeys are members of different lineages of simians, which have been separated from each other for at least 25 million years (Hoffstetter, '74; Fleagle et al., '86; Mac Fad-

Accepted April 11, 1989.

Address reprint requests to Dr. Mario Fiorani, Jr., Departamento de Neurobiologia, Instituto de Biofísica Carlos Chagas Filho, Bl. G, CCS, Ilha do Fundão, Rio de Janeiro, RJ, 21941 Brasil.

den, '87). These differences could be attributed to divergent evolution and might be characteristic of these two lineages. Nevertheless, *Macaca* and *Aotus* also differ in other respects, such as brain size, gross cortical anatomy, and visual habits. The differences so far observed could, thus, be examples of adaptative variations among genera of monkeys in both superfamilies or be a consequence of epigenetic factors in cortical development. In order to evaluate these hypotheses, we have been studying the visual areas in a diurnal New World monkey, *Cebus apella* (Gattass et al., '87; Rosa et al., '88a,b), which is similar to *Macaca fascicularis* in brain size, sulcal pattern, and certain aspects of visual behavior (Freese and Oppenheimer, '81).

In *Aotus,* MT (a list of abbreviations and their meanings adjoins Fig. 1) is a heavily myelinated visual area located in the middle temporal gyrus. It is topographically organized and receives direct projections from the striate cortex (V1) (Allman and Kaas, '71a; Lin et al., '82). The representation of the visual field in MT in *Aotus* is a first-order transformation of the whole visual field. In the macaque, several studies have demonstrated that V1 projects to a limited area in the posterior portion of the superior temporal sulcus (ST) (Zeki, '71; Lund et al., '75; Ungerleider and Mishkin, '79; Montero, '80; Rockland and Pandya, '81; Weller and Kaas, '83; Van Essen et al., '86; Ungerleider and Desimone, '86a,b). This area, referred as "motion-sensitive area of the superior temporal sulcus" (Dubner and Zeki, '71), "V5" (Zeki, '80), or "MT" (Gattass and Gross, '81; Van Essen et al., '81; Maunsell and Van Essen, '87), has a retinotopic organization variously described as "crude" (Zeki, '74), containing "multiple representations of the visual field" (Zeki, '78), "complex" (Maunsell et al., '79), and "consistent with a mosaic representation" (Van Essen et al., '81). In contrast, other studies have emphasized the existence of a continuous retinotopic organization in MT, both at local (Albright and Desimone, '87) and global levels (Gattass and Gross, '81; Maunsell and Van Essen, '87). In addition to these differences, the extent and the location of the borders of MT in the macaque have also been the object of controversy. Some authors report that MT extends beyond the heavily myelinated zone of ST (Gattass and Gross, '81; Desimone and Ungerleider, '86), while others report that it ends precisely at the border of this zone (Van Essen et al., '81, Maunsell and Van Essen, '87).

On the basis of recordings from small groups of neurons (multi-units), we report on the visual topography of area MT. MT in the *Cebus* is not located in the middle temporal gyrus; however, we will use the designation MT, which was proposed for the heavily myelinated, striate projection zone in the middle temporal gyrus of New World monkeys (Allman and Kaas, '71a; Spatz and Tigges, '72), to avoid further multiplication of names.

Preliminary reports of these results have appeared elsewhere (Fiorani et al., '85; Gattass et al., '86a).

MATERIALS AND METHODS

Cebus apella monkeys weighing between 2.8 and 4.6 kg were used. The cortex in and about MT was systematically studied with vertical electrode penetrations. The topography of the visual field representation was determined by relating the positions of receptive fields of small clusters of neurons to the locations of the corresponding recording sites in the cortex. Quantitative analysis was performed on data obtained from three animals in which MT was extensively studied. The results on the visual topography and myeloarchitecture were confirmed in five additional animals used for other studies.

The preanesthetic medication, induction, and maintenance of anesthesia, immobilization, and electrode characteristics have all been described in detail previously (Gattass and Gross, '81). Briefly, prior to the first recording session, a recording chamber and a bolt for holding the head were implanted under aseptic conditions after the administration of ketamine (50 mg/kg) and benzodiazepine (2 mg/kg). During the recording sessions, the animals were maintained under 70% nitrous oxide and 30% oxygen and immobilized with pancuronium bromide. Varnish-coated tungsten microelectrodes with impedance of about 0.5 MΩ at 500 Hz were used. For each animal a single electrode was used in all recording sessions. Vertical penetrations were made through the intact duramater in twice-weekly experimental sessions carried out over a 4-week period. The penetrations were spaced by 1.5–2.0 mm, forming a grid extending throughout area MT and adjacent areas. In each penetration, recording sites were separated by 300–500 μm.

Visual stimuli

White and colored opaque stimuli were presented on a transparent plastic hemisphere located 570 mm from the contralateral eye, under photopic illumination. The eye was focused at 570 mm by means of an appropriate contact lens (see Gattass and Gross, '81, for additional details).

Histology

The histological procedures were similar to those employed in previous work (Gattass and Gross, '81). Electrolytic lesions were made at several sites along each penetration in order to add precision in the spacing of the recording sites along each penetration. Alternate 40 μm frozen sections, either coronal or parasagittal, were stained for cell bodies with cresyl violet or for myelin with a modified Heidenhain-Woelcke stain.

Determination of the borders of MT

The borders of area MT with the surrounding areas were primarily determined on the basis of transitions in the topographical representation of the visual field revealed by reversions or discontinuities in the progressions of receptive fields recorded sequentially in the cortex. Receptive field size was also used as a parameter to determine the medial and ventral borders of MT.

Because of the large overlap of receptive fields and the scatter in the location of the receptive field centers in MT, as well as the distance between recording sites used in this study, the precision of the electrophysiological method was about 1 mm. In order to draw the complete perimeter of area MT, we studied the correspondence between electrophysiologically and myeloarchitectonically determined transitions. These myeloarchitectonic transitions, which usually ranged from 0.5 to 1 mm, were then used to delimit area MT. In each section, the borders were drawn in the center of these transitions.

Unfolding of the cortical models and visual maps

In order to obtain a "map" of the visual topography of MT for each animal, we built three-dimensional wire models of layer IV from the superior temporal sulcus at 7.5 × mag-

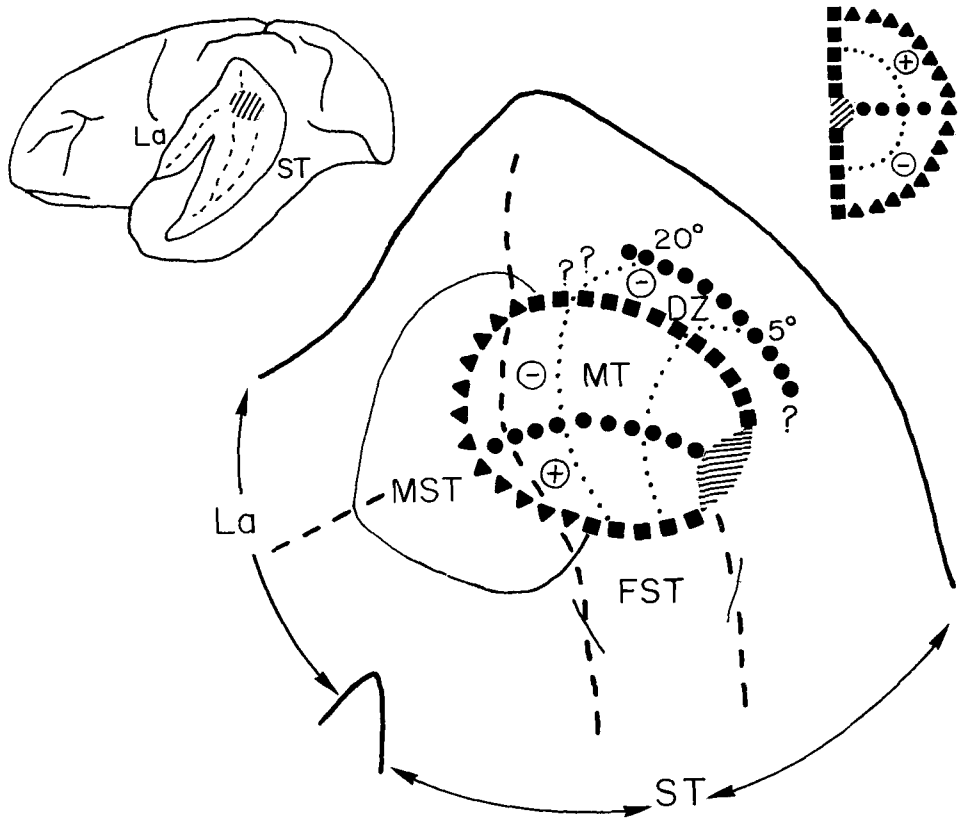

Fig. 1. Summary of the visual topography and location of MT and surrounding areas. **Upper left:** Lateral view of the *Cebus* monkey brain with superior temporal and lateral sulci partially opened. The location of visual area MT is shown in hatching. **Lower:** Enlarged view of the dorsal portion of ST showing the visual topography of MT and DZ, as well as the locations of MST and FST. The thin lines indicate myeloarchitetonic borders of MST and FST, and the dashed lines represent the main folds of the sulci. The insert in upper right is a representation of the upper (+) and lower (−) contralateral visual quadrants. The squares indicate the representation of the vertical meridian, the filled circles the representation of the horizontal meridian, the triangles the representation of the periphery, and the hatched region the representation of the fovea. The dotted lines represent isoeccentricity lines.

nification and then unfolded them, following the same procedure as Gattass et al. ('87). In these models special care was taken to align and space adjacent sections precisely. Horizontal reference needles were used as landmarks to align the wire-made contours and to calculate the correct size of the cross-linking pieces by trigonometry. Discontinuities were introduced in the maps whenever excessive distortions could be introduced by the flattening procedure. The recording sites and the myeloarchitectonic borders were projected orthogonally to the cortical surface onto layer IV in the flattened reconstructions.

In order to obtain the visuotopic map of MT for each animal, the location of the recording sites in the flattened maps and the corresponding coordinates of the receptive field centers were digitized, and maps for polar coordinates were obtained by using the interpolation algorithm proposed by Maunsell and Van Essen ('87). Logarithmic scaling was used to interpolate eccentricity values while polar angle values were interpolated linearly. Polar coordinates were interpolated between all possible pairs of recording sites to fill a grid of square bins (0.25 mm side). The array of bins con-

Abbreviations

DZ	dorsal zone (relative to MT)
DZd	densily myelinated DZ
DZp	pale myelinated DZ
ecc	eccentricity
FST	visual zone of the floor of superior temporal sulcus
HM	horizontal meridian
La	lateral sulcus
M	cortical magnification factor
MPIS	minimum point-image size
MST	medial superior temporal area
MT	middle temporal area
MTd	densily myelinated MT
MTp	pale myelinated MT
MU	multiunit
MUPIS	multiunit point-image size
RF	receptive field
SC	scatter
ST	superior temporal sulcus
V1	primary visual area
V2	second visual area
VM	vertical meridian

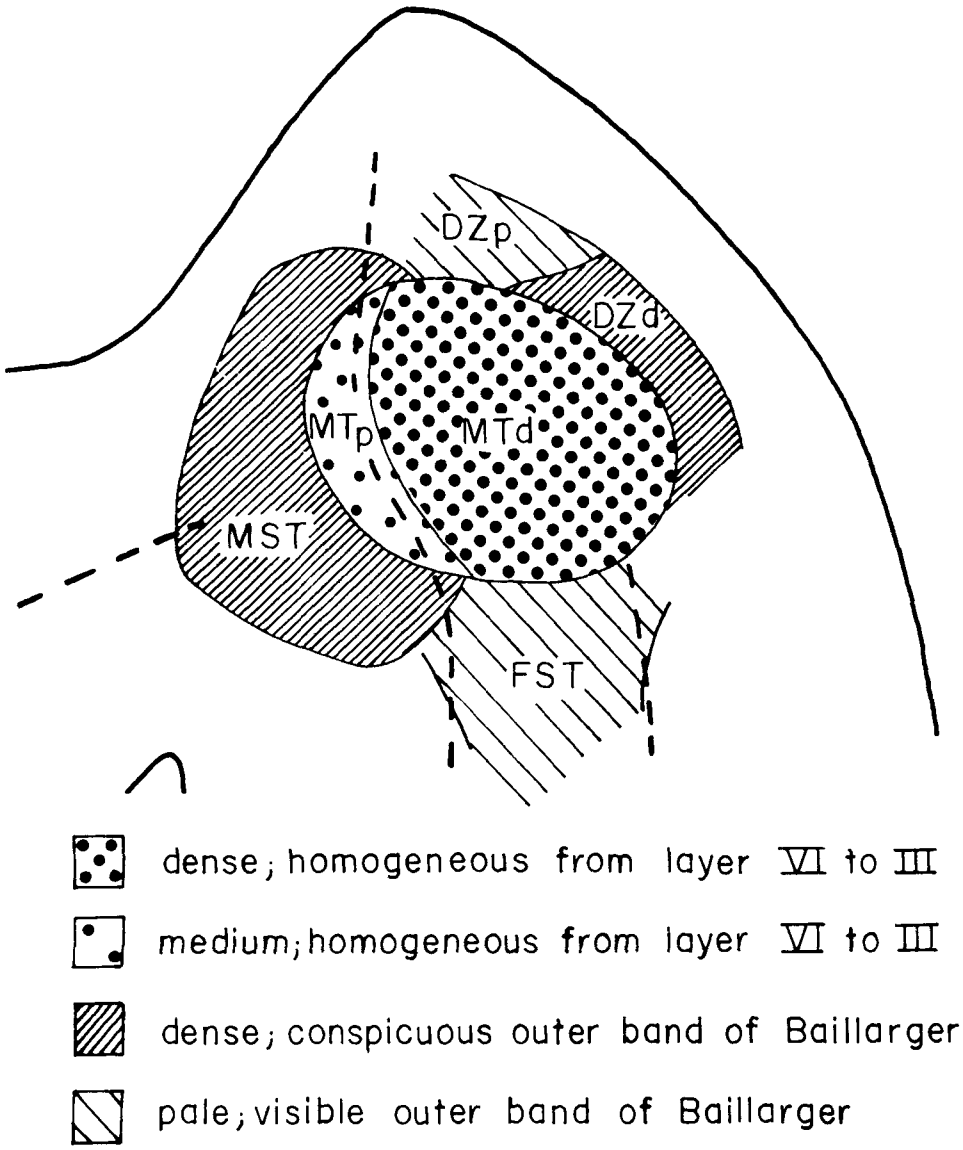

Fig. 2. Distribution of the patterns of myelination in MT and in surrounding cortex, shown in a schematic view of the unfolded dorsal portion of ST. For details, see text.

taining the average value of the coordinate of each bin was used to draw the isopolar and isoeccentric lines for each map, as shown in Figure 8. Similar maps were obtained regardless of the range of distances used for interpolation.

RESULTS

Location and overall organization

In the *Cebus*, MT is an oval area located mainly in the posterior bank of the dorsal portion of the superior temporal sulcus (Fig. 1). Our results indicate that in each hemisphere MT contains a coarse, continuous representation of the contralateral binocular segment of the visual field. The representation of the vertical meridian forms the dorsolateral, lateral, and ventrolateral borders and that of the horizontal meridian runs mediolaterally across the posterior bank of ST. The upper field is located ventrally and the lower field dorsally. The foveal representation is lateral in the posterior bank of ST. The average area of MT in four animals was 69 mm^2 (SD = 11).

MT is bordered by at least three distinct visually responsive zones (Fig. 1). Two of these zones were named, based on the similarities of their myeloarchitecture and location with those of *M. fascicularis*, as MST (Medial Superior Temporal area; Maunsell and Van Essen, '83c) and FST (the visual zone of the floor of ST; Desimone and Ungerleider, '86; Ungerleider and Desimone, '86b). MST is located in the anterior bank of ST and abuts the representation of the periphery of MT; FST is located ventrally and borders the representation of the upper vertical meridian of MT. A third area, named in this study as DZ (the visual zone dorsal to MT), is located dorsolaterally and borders the representation of the lower vertical meridian of MT.

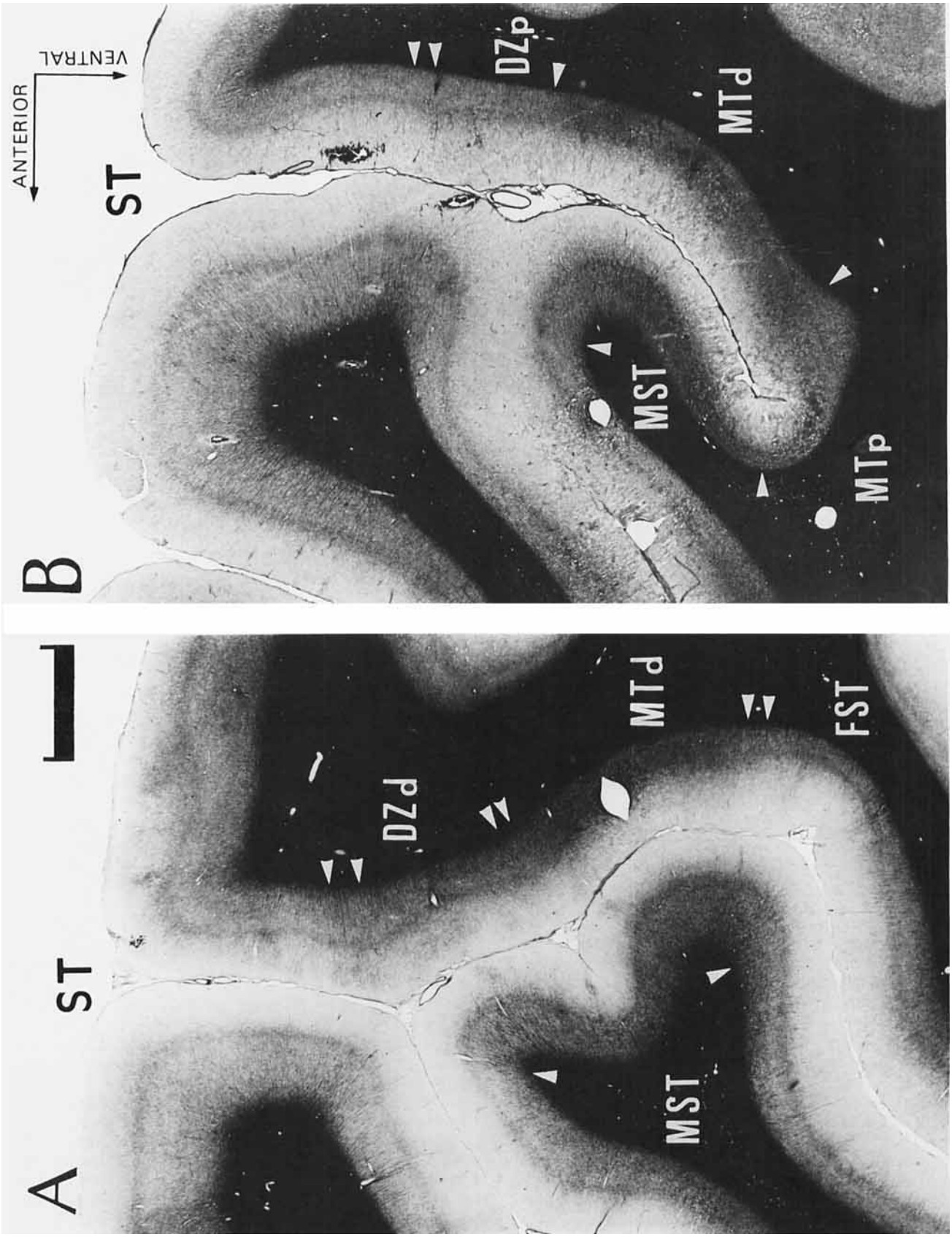

Figure 3

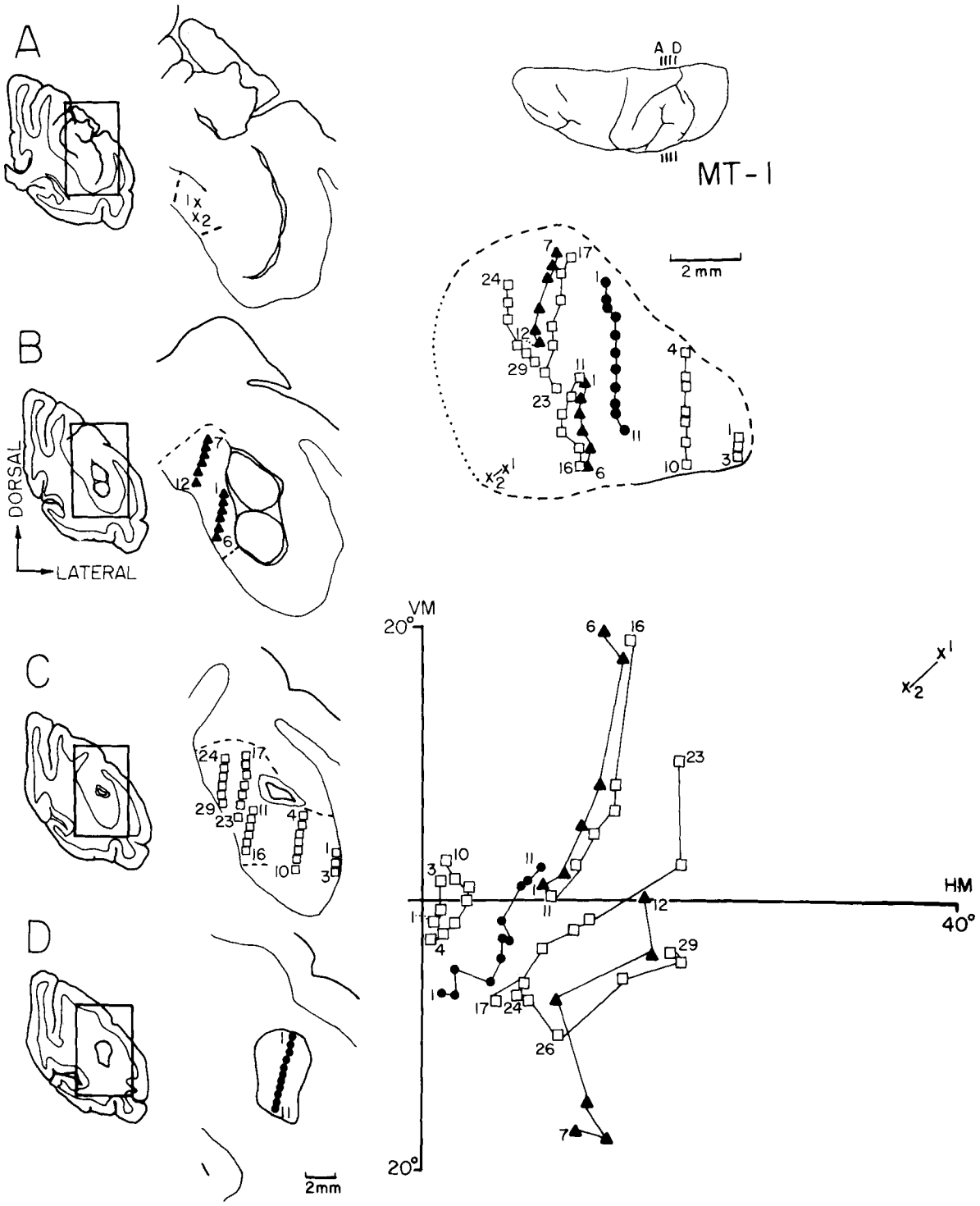

Fig. 3. Photomicrographs of myelin-stained parasagittal sections through MT and surrounding areas. **A:** Section from animal MT-2, cut at a level more lateral than **section B** from animal MT-4. Myeloarchitectonic borders are shown by arrowheads. Gradual transitions are indicated by multiple arrowheads. Calibration bar: 2 mm. For details, see text.

Fig. 4. Location of receptive field centers (**lower right**) corresponding to recording sites indicated on the enlarged views of ST from coronal sections (**A–D**) cut at the levels shown on the dorsal view of the brain (**insert**). **Upper right:** Flattened reconstruction of MT with corresponding recording sites. Note that the recording sites were located following the digitized grid (bin = 0.25 mm) used for back-transformation analysis. The dashed line is the myeloarchitectonic border of MT, the continuous line is the electrophysiological ventral border of MT, and the dotted line is the estimated medial border of MT.

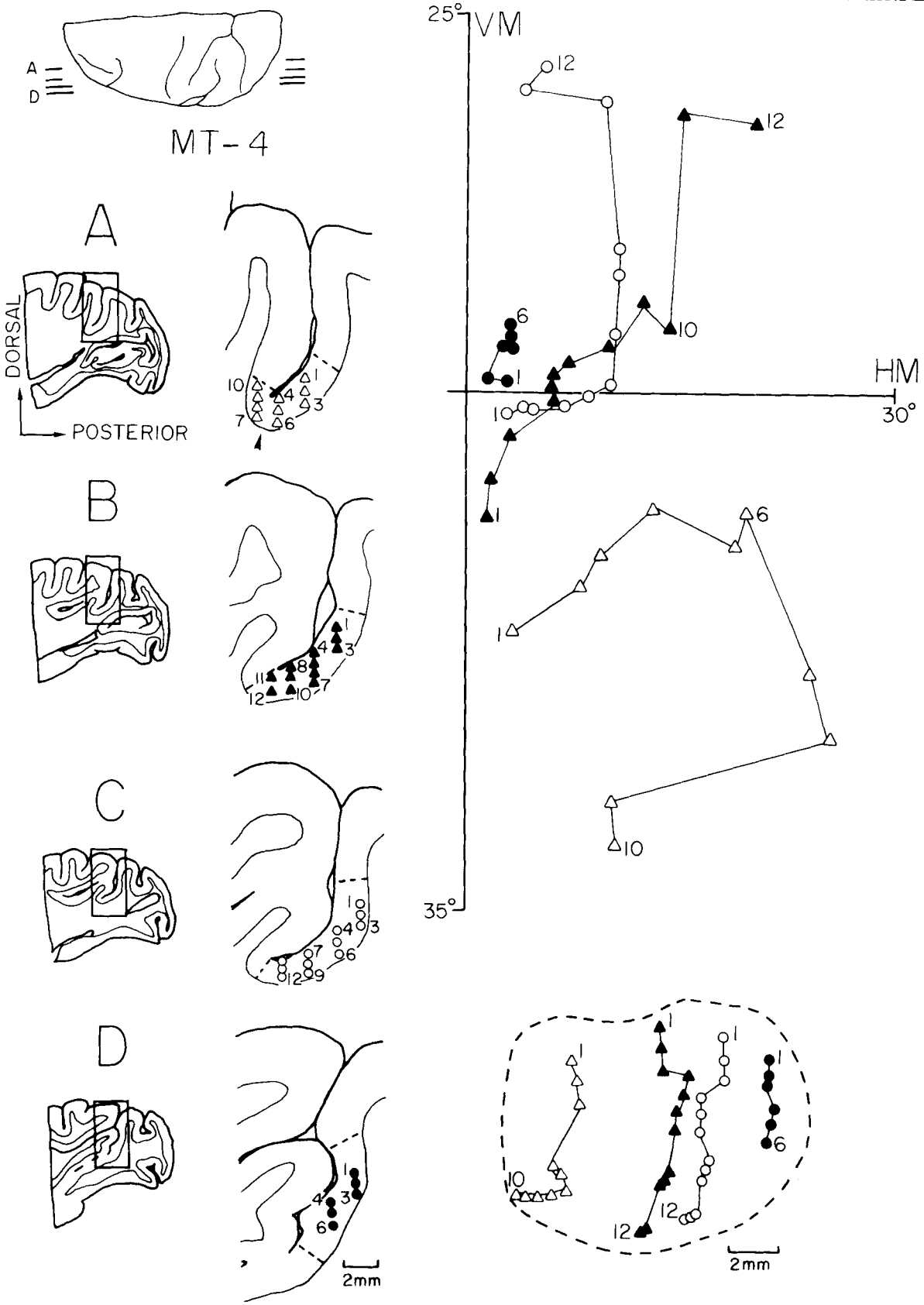

Fig. 5. Location of receptive field centers (**upper right**) corresponding to recording sites indicated on enlarged views of ST from parasagittal sections (**A–D**) cut at the levels indicated on the dorsal view of the brain (**insert**). **Lower right:** Flattened reconstruction of MT with corresponding recording sites. Dashed line is the myeloarchitectonic border of MT. Arrowhead in section A points to the myeloarchitectonic transition between MTd and MTp.

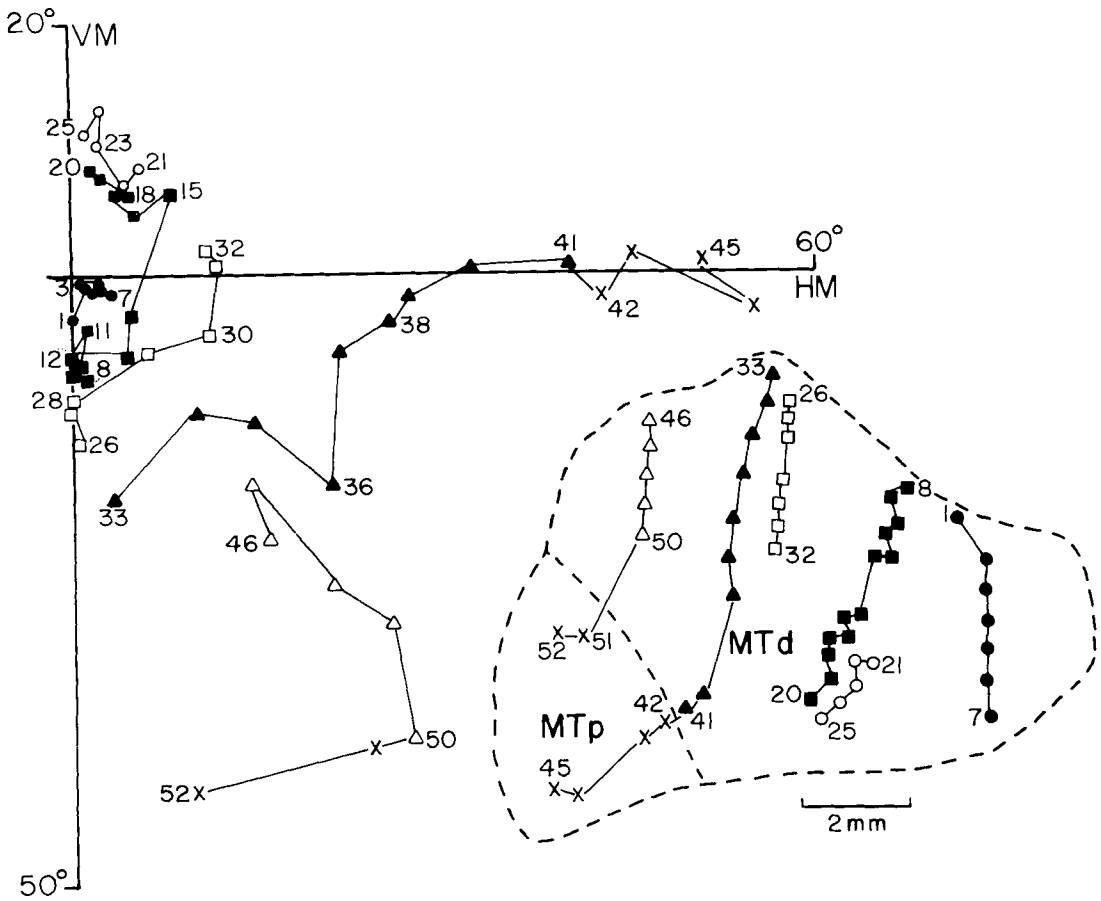

Fig. 6. Location of receptive field centers (**left**) corresponding to recording sites indicated on a flattened reconstruction of area MT (**right**) of animal MT-2. Each sequence of recording sites was reconstructed from several penetrations. Dashed lines indicate myeloarchitectonic borders. For details, see text.

Myeloarchitecture of dorsal ST

In dorsal ST we distinguish at least six myeloarchitectonic zones: MTd (densely myelinated MT), MTp (pale myelinated MT), MST, DZd (densely myelinated DZ), DZp (pale myelinated DZ), and FST. The location of these zones is shown in a schematic flattened map of dorsal ST in Figure 2.

MTd is located in the posterior bank of ST and shows a dense and homogeneous pattern of fibers extending from layer VI to the bottom of layer III (Fig. 3A,B). In this region the outer limit of the outer band of Baillarger is not sharply defined. Anterior and medial to MTd, in the fold between the posterior and anterior banks of ST, we find a region with a homogeneous pattern similar to that of MTd but less densely myelinated, named MTp (Fig. 3B). The average areas of MTd and MTp in four animals were 58 (±3) mm^2 and 11 (±7) mm^2, respectively.

Adjacent to MTp, in the anterior bank of ST and in the posterior portion of the lateral sulcus, there is another heavily myelinated zone, MST, which differs from MTd by showing a conspicuous outer band of Baillarger (Fig. 3A, B). A similar pattern of myelination is observed in another region, DZd, located dorsolateral to MTp, in the posterior bank of ST (Fig. 3A).

Medial to DZd and bordering MTd dorsally there is another strip of cortex, DZp, with a visible outer band of Baillarger and pale myeloarchitecture when compared with that of the surrounding regions (Fig. 3B). Ventral to MTd, in the floor of ST, there is a region, FST, with a pattern of myelination similar to that observed in DZp (Fig. 3A). However, in most animals FST shows a more conspicuous outer band of Baillarger than that of DZp. While it is always possible to identify MTd and DZd, MTp and DZp cannot be clearly distinguished in all animals.

Visual topography of MT

Figures 4 and 5 show the locations of recording sites in MT, reconstructed from coronal and parasagittal sections, respectively, and of the corresponding receptive field centers in two animals. Note that the central visual field is represented laterally in ST (Fig. 4, section C, sites 1–3; Fig. 5, section D), while the periphery is represented more anterior and medially (Fig. 5, sites A5–10 and B11,12). The upper quadrant is represented ventrally and the lower quadrant dorsally (see, for example, Fig. 4, section C, sites 4–10 and 17–23). In all animals, there are irregularities in the visuotopy, a certain degree of overlap occurring in the representation of receptive field centers at adjacent sequences of

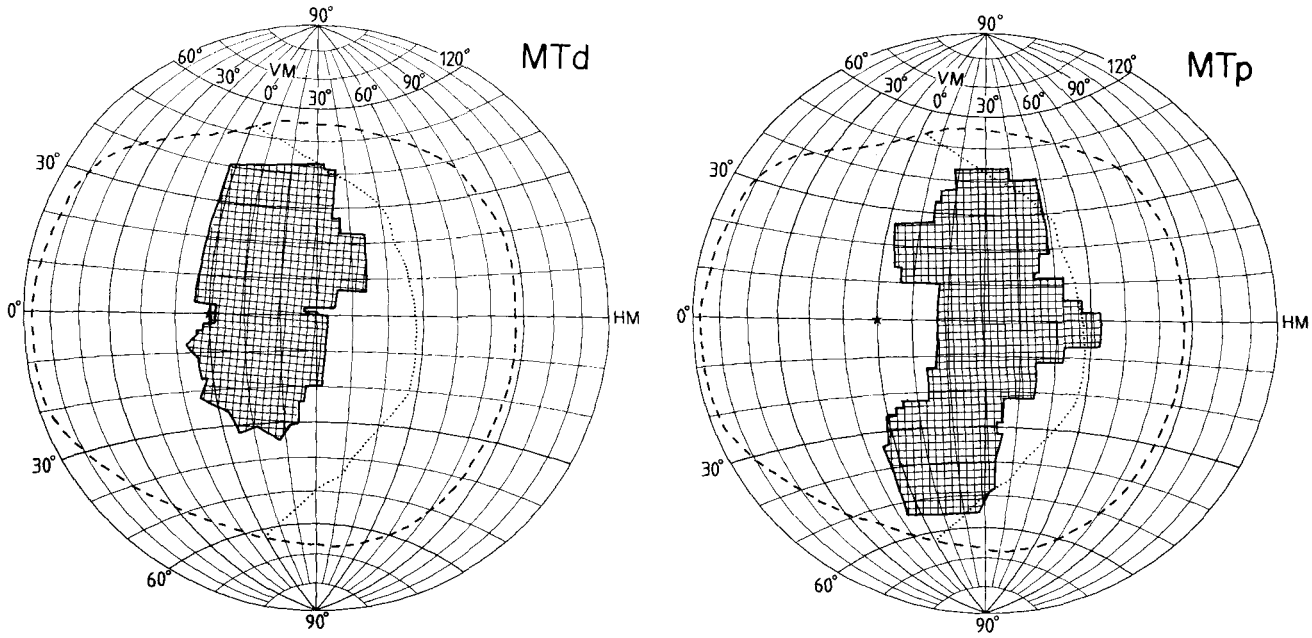

Fig. 7. Extent of the visual field represented in MTd and MTp. The shaded regions outline all receptive fields recorded in MTd (**left**) and MTp (**right**) in eight animals. Dashed line is the mean extent of the monocular field of vision in three *Cebus* monkeys, studied as described in Gattass et al. ('87). The dotted line represents the temporal border of the binocular visual field, and the star the center of gaze.

recording sites (e.g., Fig. 5, sections B and C). On the other hand, evidence for the regularity of representation abounds. For instance, closely located sites represent the same portions of the visual field (Fig. 4B1–6 and C11–16).

Figure 6 shows the locations of receptive field centers and recording sites in a flattened reconstruction of MTd and MTp from another animal studied in the parasagittal plane. Inasmuch as no topographic discontinuities were observed at the transition between MTd and MTp, and the region of the visual field represented in MTp does not include the central 10–20°, which are represented in MTd (Fig. 7), we have chosen to consider MT as a single area, coextensive with these two myeloarchitectonic regions (see also Fig. 5, section A). Note that the region of the visual field represented in both MTd and MTp does not include the monocular crescent. We have never observed field centers beyond 60° eccentricity.

Details of the visuotopic organization of MT were evaluated in maps showing isoeccentric (Fig. 8—upper) and isopolar (Fig. 8—middle) lines drawn from arrays of interpolated coordinates, as described in Materials and Methods. In spite of individual variability (see below), the overall visuotopic organization is consistent among animals.

In order to visualize the degree of visuotopic orderliness and the existence of overrepresentations of sectors of the visual field in MT we projected onto the visual field a grid defined by an array of interpolated coordinates corresponding to equally spaced points in the cortex (Fig. 9), following the procedure (back-transformed map) described by Maunsell and Van Essen ('87). As previously described (Schwartz, '80; Van Essen et al., '84; Maunsell and Van Essen, '87), a precisely organized visual map, with no rerepresentation of portions of the visual field, would transform a square grid on the cortex onto an orderly cobweb pattern in the visual field. This analysis showed an indi vidual variability in the degree of visuotopic orderliness in MT, with a considerable organization in animal MT-4 and a more irregular organization in MT-2. Although no consistent biases towards rerepresentations could be observed, the back-transformed maps of animals MT-1 and MT-2 suggest a tendency for greater representation of a sector of the visual field located away from both the horizontal and vertical meridians. In conclusion, the evidence favors the presence in MT of a single and continuous representation of the binocular visual field.

Cortical magnification factor

The cortical magnification factor (M), i.e., the ratio of the cortical distance between two recording sites, in millimeters, and the corresponding displacement of field centers, in degrees (Daniel and Whitteridge, '61), was determined based on discrete measurements in MT. The variation of M with eccentricity was evaluated with the aid of an automatic system which calculates M by using all possible pairs of recording sites located in the range of 0.5–3 mm from each other, based on digitized flattened maps of layer IV of MT. The resulting values of M were attributed to the geometric mean of the eccentricities of the pairs of receptive fields. Figure 10A–C shows the plots of the cortical magnification factor as a function of eccentricity calculated from data obtained in three animals. The best-fitting power function for the pool of data (Fig. 10D) is given by the function

$$M = 1.67 \times (ecc)^{-0.85} \quad (r = -.63; n = 1{,}534) \qquad (1)$$

In this function, ecc is the eccentricity and r is the coefficient of correlation. The small correlation of this regression reflects interanimal variability, inasmuch as the fitting of the data was considerably better for each individual case. No statistical difference was found between the local measurements of M in the representations of the upper and

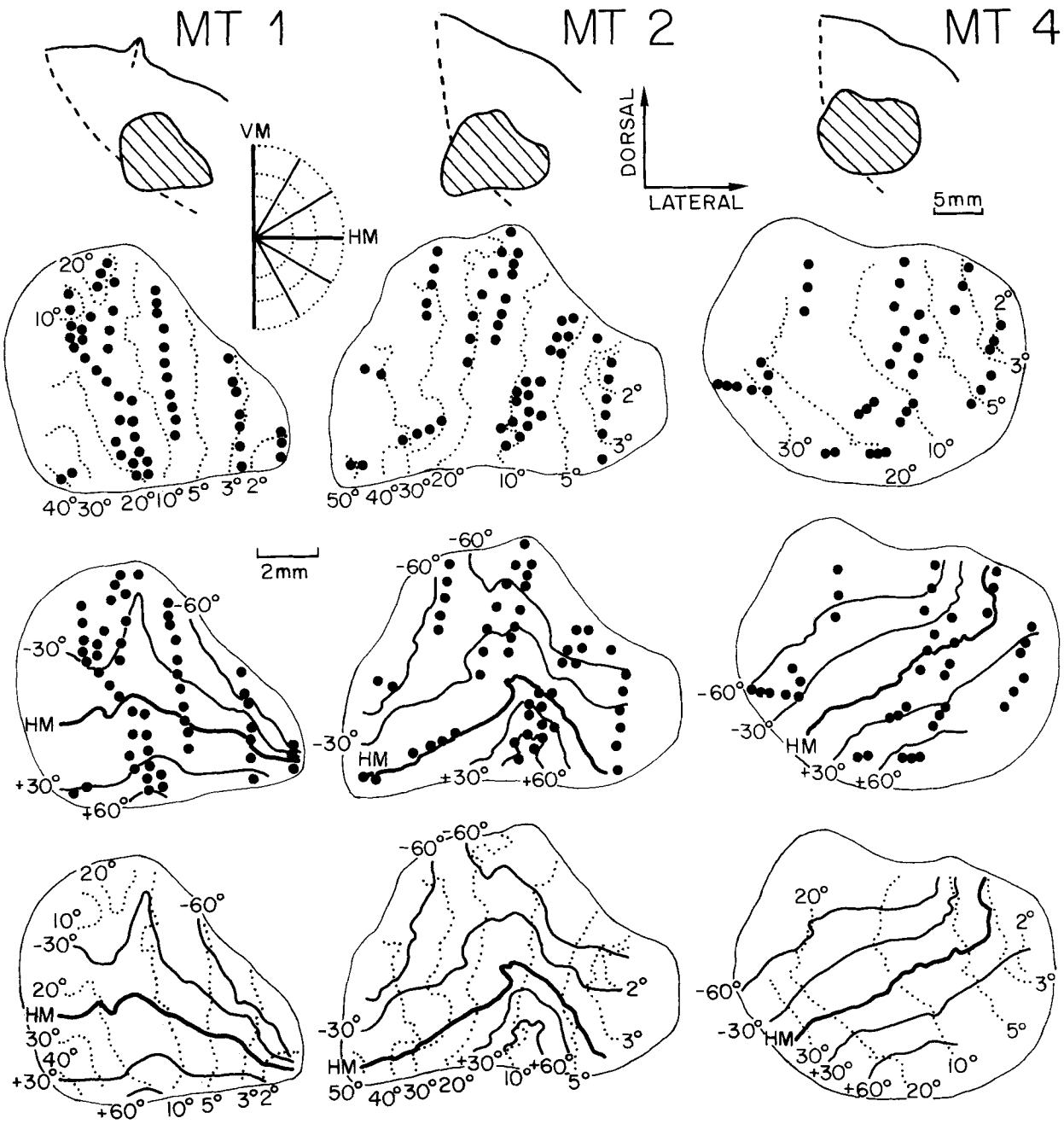

Fig. 8. Interpolated visual maps of MT in three animals. Interpolated isoeccentricity lines (**upper**) and isopolar lines (**middle**) were combined to form the visual maps of MT (**lower**). **Upper inserts:** Show the location of MT (shaded) in ST. Dashed lines represent the fold between the banks of ST. For details, see text.

lower quadrants, either in the pooled data ($P > .4$) of in that from each animal. We also studied the magnification functions for isopolar and isoeccentric dimensions in the visual maps, and no statistical differences were found between these data ($P > .8$).

Receptive field size

The variation of multiunit receptive field size with eccentricity in MT is shown in Figure 11. As in other visual areas, in MT the receptive field size, i.e., the square root of the receptive field area, grows markedly with increasing eccentricity. In order to compare this variation with that in other visual areas a straight line was fitted to the pooled data with the method of least squares. Field size varies with eccentricity following the function

$$\sqrt{\text{RF area}} = 2.45 + 0.39(\text{ecc})(r = .79; n = 161) \quad (2)$$

As shown in Figure 11, this function (dashed line) describes well the data except for the centralmost receptive

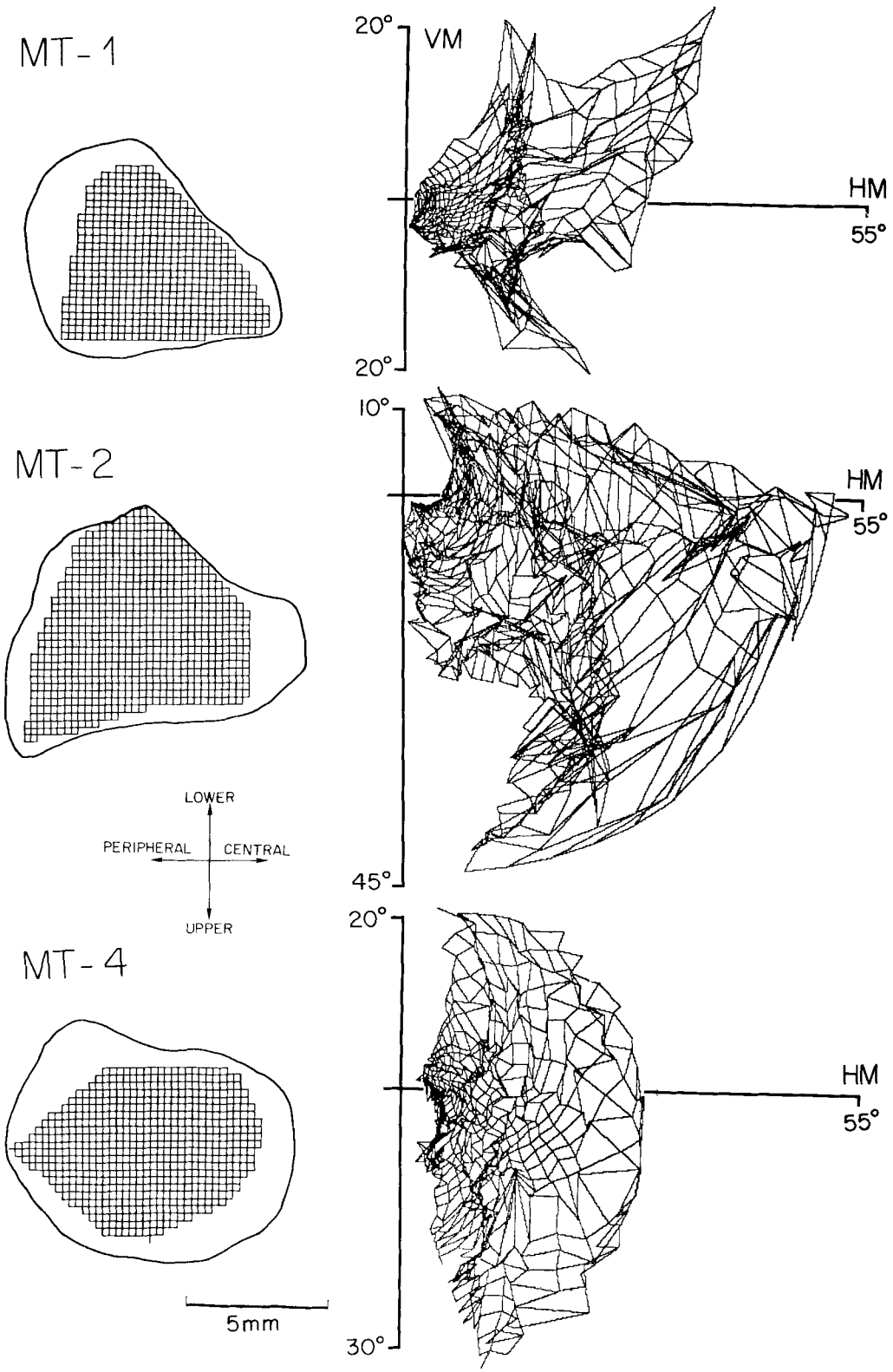

Fig. 9. Back-transformed maps for the same animals illustrated in Figure 8. The grids representing the interpolation matrices of coordinates (**left**) were projected onto the representation of the visual hemifield (**right**). The matrix for each animal was defined in order to include all recording sites illustrated in the previous figure.

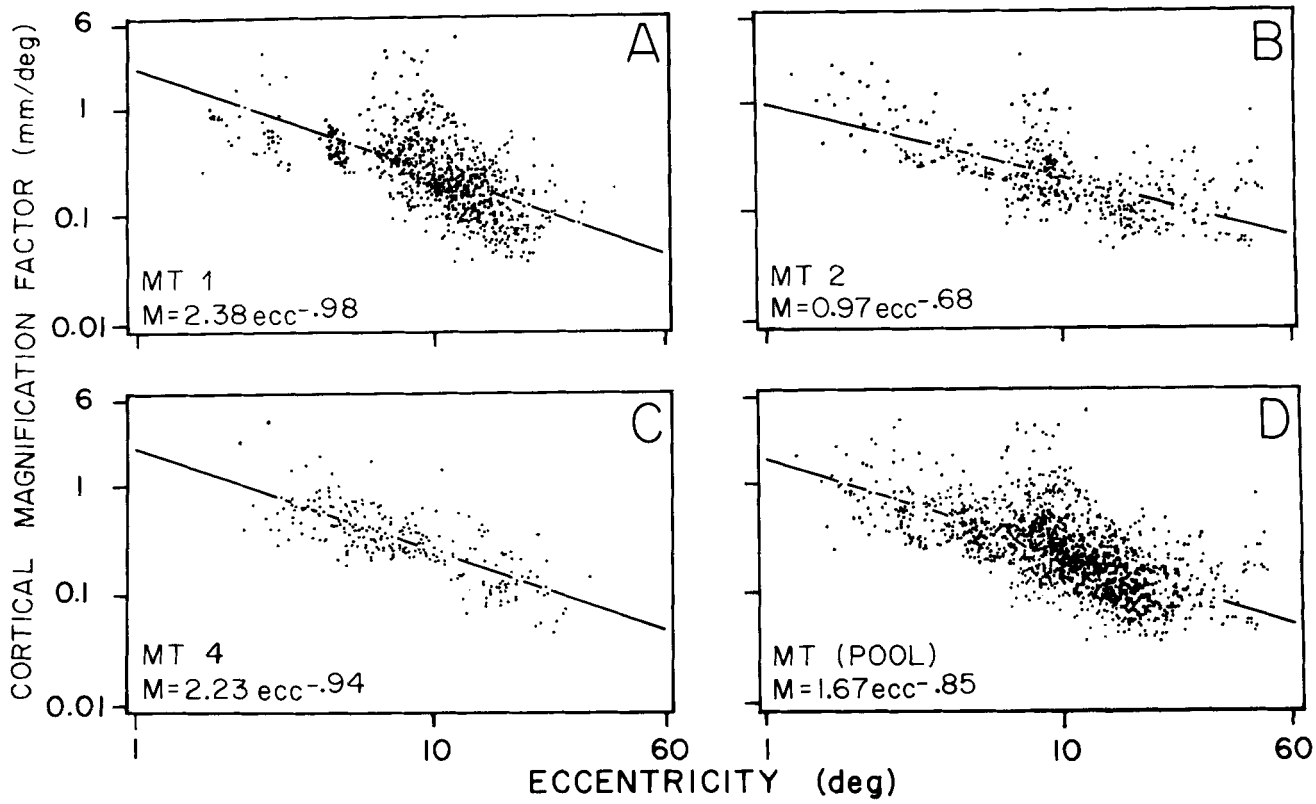

Fig. 10. Cortical magnification factor in MT as a function of eccentricity. **A–C:** Power functions fitted to the data from animals MT-1, MT-2, and MT-4. **D:** Power function fitted to the pool of data from the three animals.

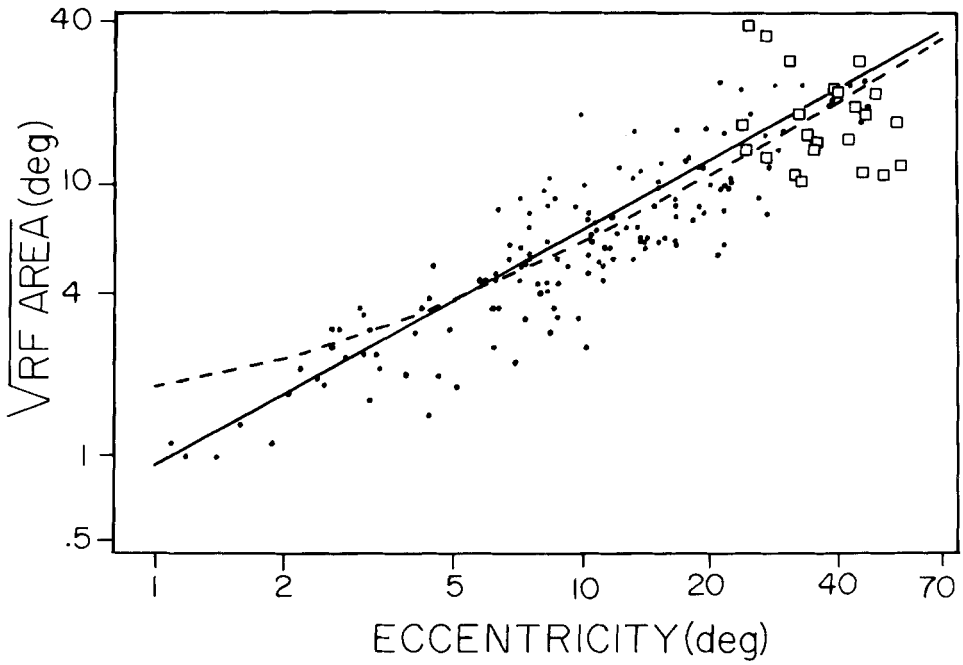

Fig. 11. Receptive field size as a function of eccentricity in MTd (dots) and MTp (squares). Linear (dashed) and power (continuous line) functions were fitted to the data from three animals.

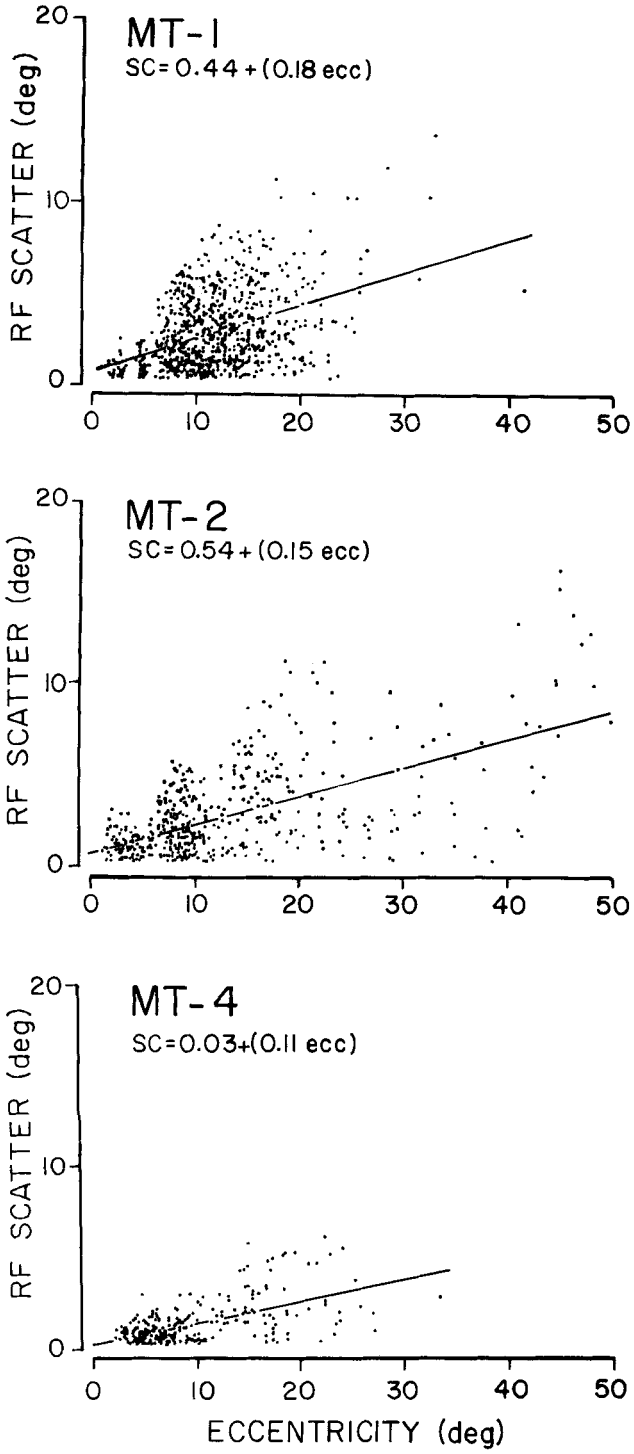

Fig. 12. Scatter in multiunit receptive field position as a function of eccentricity for three animals. For details, see text.

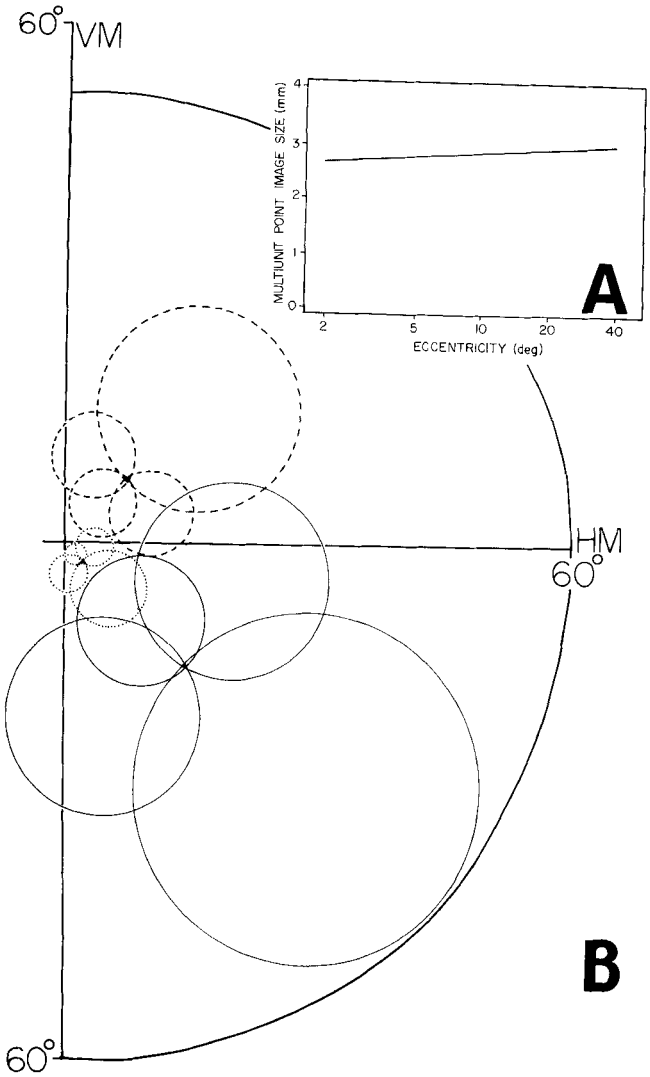

Fig. 13. **A:** Multiunit point-image size as a function of eccentricity in MT, based on data pooled from three animals. **B:** Schematic representations of aggregate receptive fields in MT. Dotted fields include a point at 3° eccentricity, dashed fields include a point at 10° eccentricity, and continuous line fields include a point at 20° eccentricity. For details, see text.

fields, which are overestimated. A better fit was obtained with a power function (Fig. 11, continuous line) expressed by the following equation:

$$\text{RF area} = 0.99(\text{ecc})^{0.78} \quad (r = .88) \qquad (3)$$

Note that receptive fields from both MTd (dots) and MTp (squares) are adequately described by this function.

These equations were obtained based on data from four animals. However, there was considerable individual variation. For example, the slopes of the linear functions for data from different animals obtained with different electrodes varied from 0.36 (MT-2) to 0.68 (MT-1).

Multiunit receptive field scatter

In order to evaluate the precision of the visuotopic organization in MT we estimated the scatter in the position of receptive field centers as a function of eccentricity. In topographically organized visual areas it is possible to quantify the scatter based on the magnification factor. If one knows the distance between two receptive field centers at a given eccentricity, as well as the expected distance obtained from the magnification function, one can define the associated scatter as the absolute value of the difference between the expected and the observed distances between the field centers. Assuming that the scatter of one receptive field is not

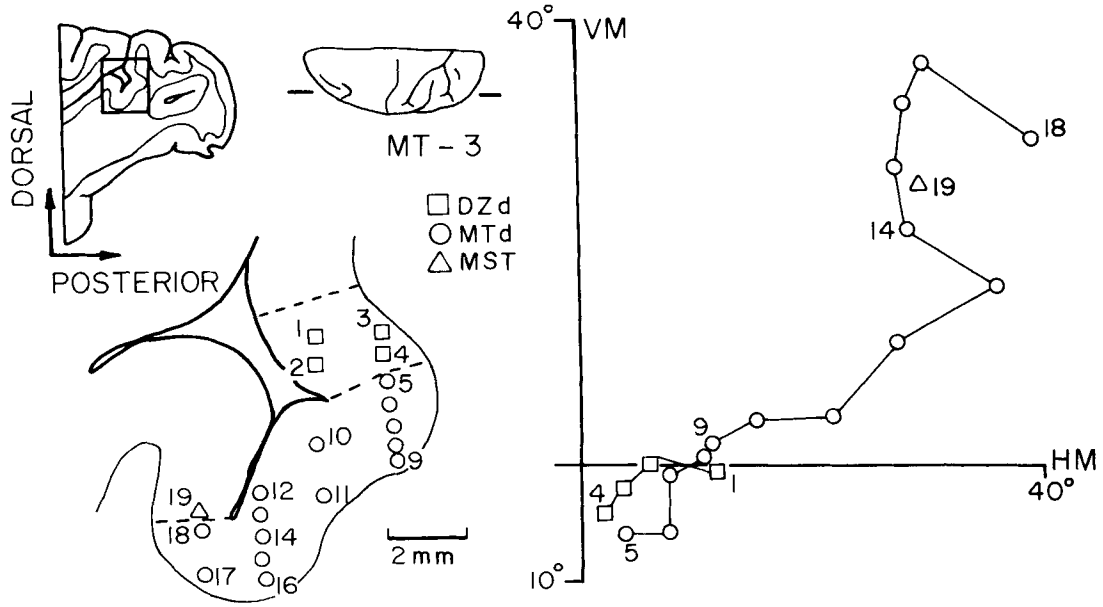

Fig. 14. Location of receptive field centers (**right**) corresponding to recording sites (**lower left**) in MT and surrounding areas shown in a parasagittal section cut at the level indicated in the dorsal view of the brain. Animal: MT-3.

related to the scatter of other receptive fields, that is, that there is no covariance between them, then the individual scatter is half of the associated one.

The scatter in the position of receptive field centers in MT was quantified based on the inverse of the magnification factor (1/M), which is expressed in degrees per millimeter. In MT of the *Cebus*, as in V1 of the macaque (Talbot and Marshall, '41; Hubel and Wiesel, '74), 1/M varies with eccentricity approximately following a linear function. In order to calculate the associated scatter in degrees, we initially multiplied the distance between each data point and the regression line (deg/mm) by the distance (mm) between the corresponding recording sites. This multiplication is necessary inasmuch as for the calculation of 1/M we have divided the associated scatter by the cortical distance. Finally, the associated scatter of each pair of points was divided by two, assuming half the total scatter to each point. Figure 12 shows the variations of the scatter with eccentricity and the best-fitting linear function for animals MT-1, MT-2, and MT-4. The regression lines give the values of the mean standard error of the receptive field position at each eccentricity. These values are good estimates of one standard deviation of the variation in receptive field positions. No statistical differences were found between isopolar and iso-eccentric scatter or between upper and lower quadrant scatter.

The size of the cortical region activated by a punctiform visual stimulus, i.e., the point image size (McIllwain, '76), has been calculated by multiplying the aggregate field size by the magnification factor at each eccentricity (Dow et al., '81; Albright and Desimone, '87). In this study we have estimated the multiunit point image size (MUPIS) by multiplying the aggregate multiunit field size, i.e., the vectorial sum of mean multiunit field size and multiunit receptive field scatter (4 standard deviations), by the magnification factor at each eccentricity. Figure 13A shows the variation of the MUPIS with eccentricity in MT based on data pooled from three animals. MUPIS curves for each animal were also nearly constant. The mean MUPIS in these cases ranged from 2.5 mm to 4.5 mm.

Due to the large size of the receptive fields and to the scatter in receptive field position in MT, a given point in the visual field is included by aggregate fields with centers located widely apart in the visual field, as illustrated in Figure 13B. For example, a point at 10° eccentricity is included in aggregate fields with centers ranging from 6.5° to 22° in eccentricity. As expected from the MUPIS function (Fig. 13A), this isopolar displacement in the visual field corresponds to a linear displacement in the surface of MT of about 3 mm (based on integration of Eq. [1]). Note that if this point is located at 45° polar angle, it is included by aggregate fields which extend to both the horizontal and the vertical meridians, regardless of the eccentricity (Fig. 13B). It is also noteworthy that an aggregate field centered at the 40° iso-eccentricity extends to the peripheral limits of the binocular field of vision. These data suggest that the coarseness of the visual topography of MT may be related to the large receptive fields observed in this area.

Interanimal variability

In all animals studied MT is located mainly in the posterior bank of ST, as illustrated in Figure 8 (upper inserts). The orientation of the representation of the horizontal meridian relative to the posterior border of ST varies from animal to animal, as did the extent of cortex representing the upper and the lower visual quadrants. The visual maps of two animals (MT-1 and MT-2) showed a compressed representation of the upper quadrant relative to that of the lower quadrant, although no statistical difference was found between the M functions for the upper and lower quadrants. In contrast, in one animal (MT-4) the extent of cortex representing the upper and lower quadrants was similar.

In each animal, the extent of the visual field included by the external borders of the most peripheral receptive fields

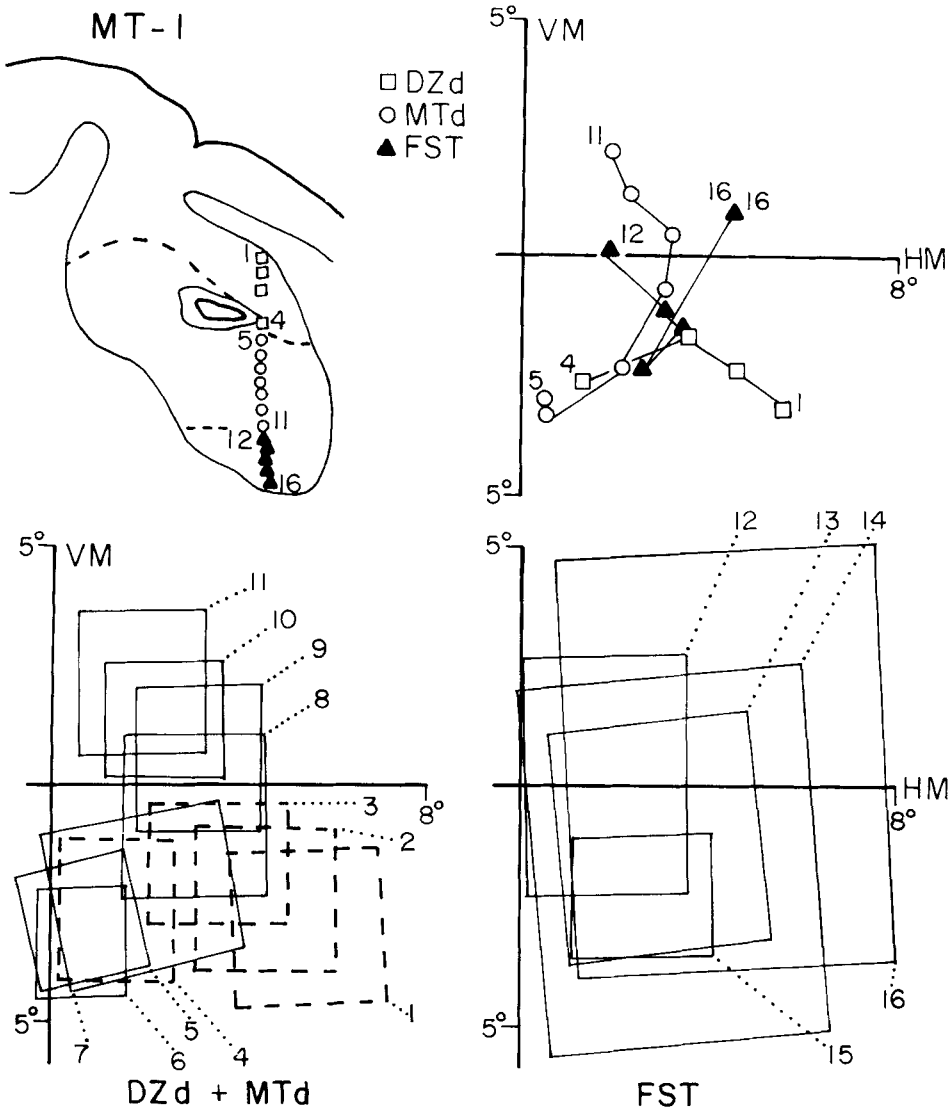

Fig. 15. Location of receptive fields (**lower**) and receptive field centers (**upper right**) in DZ, MT, and FST, corresponding to recording sites illustrated in a coronal section through ST (**upper left**). This section corresponds to section C in Figure 4.

reached the limits of the binocular field. However, depending on the variation of receptive field size with eccentricity, the position of the most eccentric receptive field centers varied considerably among animals. The most peripheral receptive field centers in animals with large peripheral receptive fields reached smaller values of eccentricity (35°, MT-1) than those in animals with small peripheral receptive fields (55°, MT-2). A similar variability was found in relation to the proximity of receptive field centers to the VM (compare back-transformed maps of animals MT-1 and MT-2 in Fig. 9).

Areas bordering MT

Dorsolaterally MT is bordered by DZ, an electrophysiologically defined zone which encompasses both DZd and DZp. This border is characterized by a reversion in the progressions of receptive field locations corresponding to sites recorded sequentially across it. As shown in Figures 14–16 the topographical transitions at the MT/DZ border coincide with the representation of regions of the visual field close to the lower vertical meridian, up to an eccentricity of 20°. The transitions in the region of representation of the central 5–10° (Figs. 14, 15) are coincident with the myeloarchitectonic borders between MTd and DZd, while the transitions in the periphery coincide with the myeloarchitectonic border between MTd and DZp (Fig. 16). Thus, although myeloarchitectonically heterogeneous, DZ may contain a single, coarse representation of the lower quadrant (Fig. 17).

MST surrounds the peripheral representation of MT and contains the representation of both the upper and lower visual quadrants (Fig. 18). A sequence of receptive fields recorded across the MT/MST border is illustrated in Figure 16. A change in the progression of receptive field centers, which coincides with an increase in receptive field size as well as with a myeloarchitectonic border, is seen between fields 15 and 16 in Figure 16.

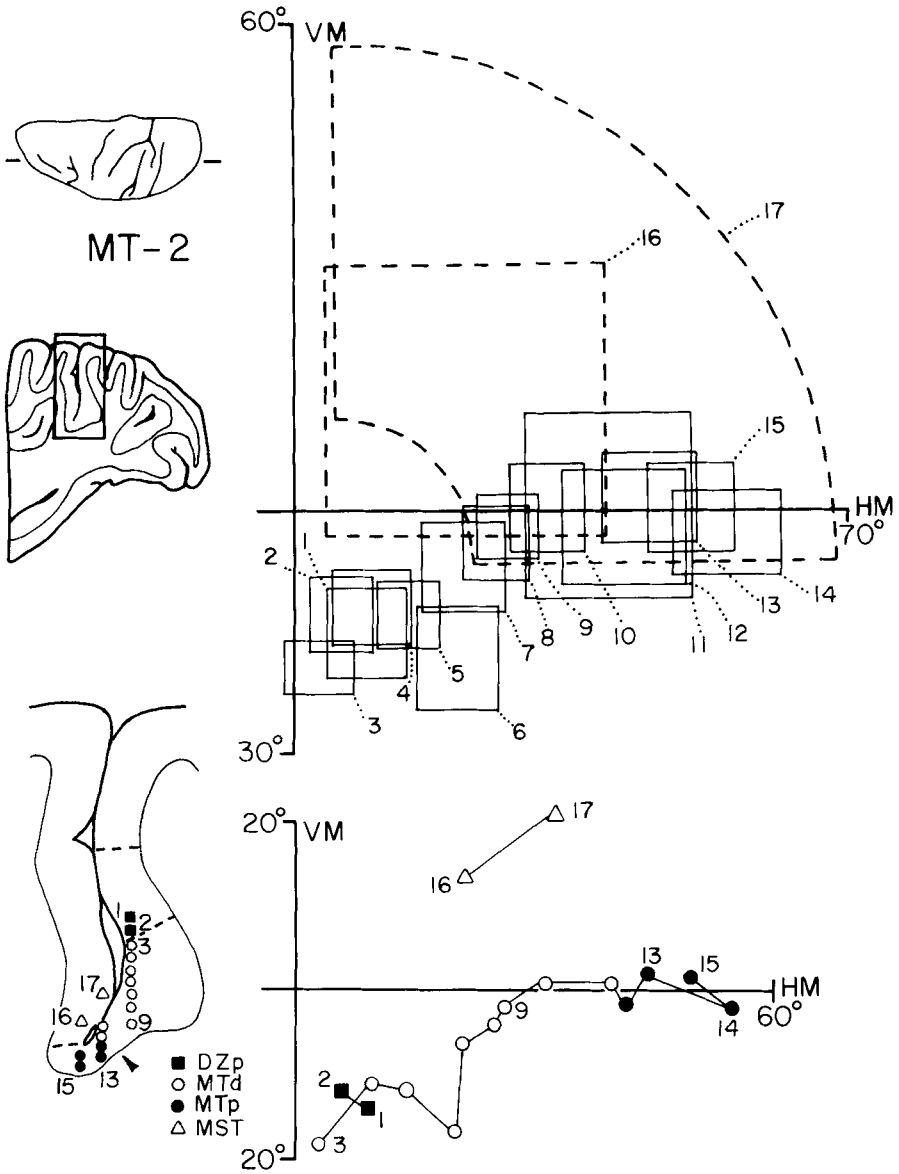

Fig. 16. Location of receptive fields (**upper right**) and receptive field centers (**lower right**) in DZ, MT, and MST, corresponding to recording sites indicated in a parasagittal section cut at the level shown in the dorsal view of the brain (**upper left**). Dashed lines in the section are myeloarchitectonic borders and the arrowhead indicates the myeloarchitectonic transition between MTd and MTp. Animal: MT-2.

Ventral to MT, in the floor of ST, there is a myeloarchitectonically distinct visually responsive zone, FST. In general, at a given eccentricity receptive fields in this zone are larger than those in MT and DZ and include both the upper and the lower visual quadrants (Fig. 15).

DISCUSSION

Extent of MT

In this study we conclude that MT is coextensive with two myeloarchitectonically distinct areas. Several authors have shown that the myeloarchitectonic pattern may vary within a single cortical area (Allman and Kaas, '71a; Sanides, '72; Gattass and Gross, '81; Rosa et al., '88b). Thus, functionally distinct areas may not always be morphologically homogeneous. Therefore, the myeloarchitectonic differences observed between MTd and MTp do not rule out per se their inclusion within a single visual area. As shown in the Results, these regions contain a single representation of the binocular visual field, showing no topographic discontinuities or reversions coincident with the myeloarchitectonic border which separates MTd from MTp.

Although we made attempts to study the boundary between MT and MST we did not find a representation of the monocular crescent in MT. However, we cannot rule out the possibility of a representation of the monocular crescent in MT, inasmuch as if one takes into account the large size of receptive fields and the small values of cortical magnification in the representation of the periphery, one is led to conclude that a strip of cortex less than 0.8 mm wide would be enough to represent the whole monocular crescent.

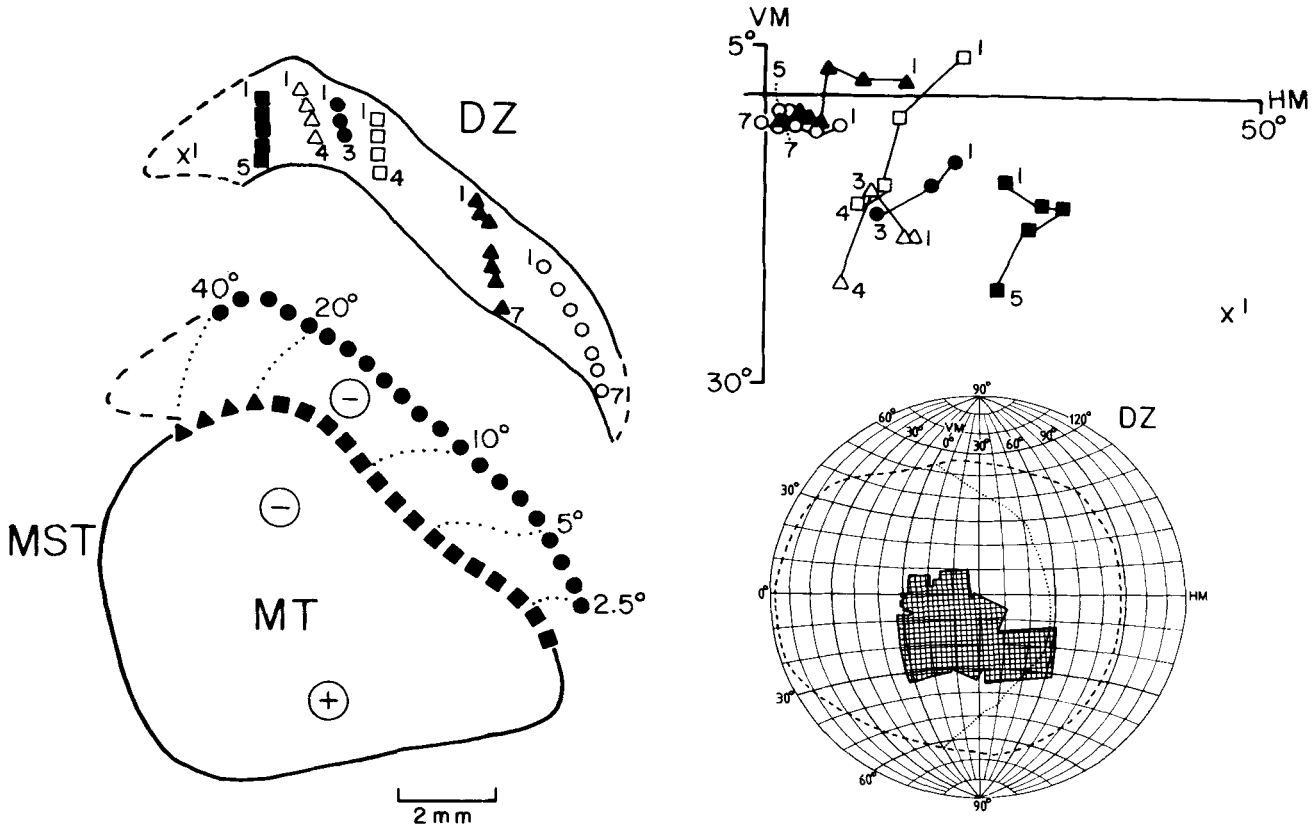

Fig. 17. Visual topography of DZ. **Upper left:** Flattened reconstruction of DZ with recording sites indicated. Continuous outline shows the region in which either the myeloarchitectonic or the electrophysiological borders of DZ were determined, and dashed lines show estimated borders. **Upper right:** Locations of receptive field centers in DZ. **Lower left:** Interpolated representation of the lower visual quadrant in DZ and its relationship to MT. Symbols as in Figure 1. **Lower right:** Extent of the visual field (shaded) represented in DZ in this animal (MT-1). See also legend to Figure 7.

Cortical magnification factor, scatter, and point-image size

In this study cortical magnification factors were obtained by a method which differs from others previously described (Gattass and Gross, '81; Albright and Desimone, '87; Gattass et al., '87; Maunsell and Van Essen, '87). In order to access the precision of this method we have also calculated M between sites located in a single plane of section, following the procedure used by Gattass and Gross ('81), as well as on three-dimensional models of layer IV, according to the procedure described by Gattass et al. ('87). The equations obtained with all methods had similar slopes and intercepts.

The equation relating M to eccentricity for animal MT-4 (Fig. 10C) predicts a surface area of 69 mm^2 for the representation of eccentricities from 2 to 60° in MT, which is in good agreement with the measurements made on flattened maps. The surface area of MT in the other animals was not estimated based on M due to the asymmetry of the representations of the lower and upper quadrants observed in these animals.

In this study we calculated the local scatter in multiunit receptive field positions in MT by using a method different from the one used by Albright and Desimone ('87). In spite of the different methods the amount of scatter observed in the *Cebus* (Fig. 11) is very similar to the that observed in the *Macaca* (Albright and Desimone, '87). In both species the scatter, in degrees, is approximately 15% of the eccentricity value. Inasmuch as receptive field size increases with increasing eccentricity, we have examined the relationship between scatter and receptive field size at various eccentricities. As in the macaque (Gattass and Gross, '81; Maunsell and Van Essen, '87), the ratio of scatter to field size does not vary with eccentricity, and the absolute value of scatter is usually smaller than half the field size.

Taking into the account the estimated scatter we were able to calculate multiunit point size (MUPIS) for MT. Previous work from this laboratory has calculated the variation of minimum point size with eccentricity (MPIS) for V1 (Gattass et al., '87). Thus, for the sake of comparison, we have also calculated a MPIS function for MT, and we found that, as MUPIS, it was nearly constant with eccentricity. The mean value of MPIS for MT of *Cebus* is 1.4 mm. In contrast, in V1 MPIS decreases markedly with eccentricity (Rosa et al., '88b), suggesting an interesting question: Why is the function relating MPIS with eccentricity nearly constant for MT, while it decreases markedly with increasing eccentricity for V1? Schein and de Monasterio ('87) have proposed that the variation of point-image size with eccentricity in V1 results from mapping of both magno- and parvicellular visual "channels" in this area. Although some of the assumptions of Schein and de Monasterio's model have recently been questioned (Livingstone and Hubel, '88), the subject of peripheral scaling and different functional chan-

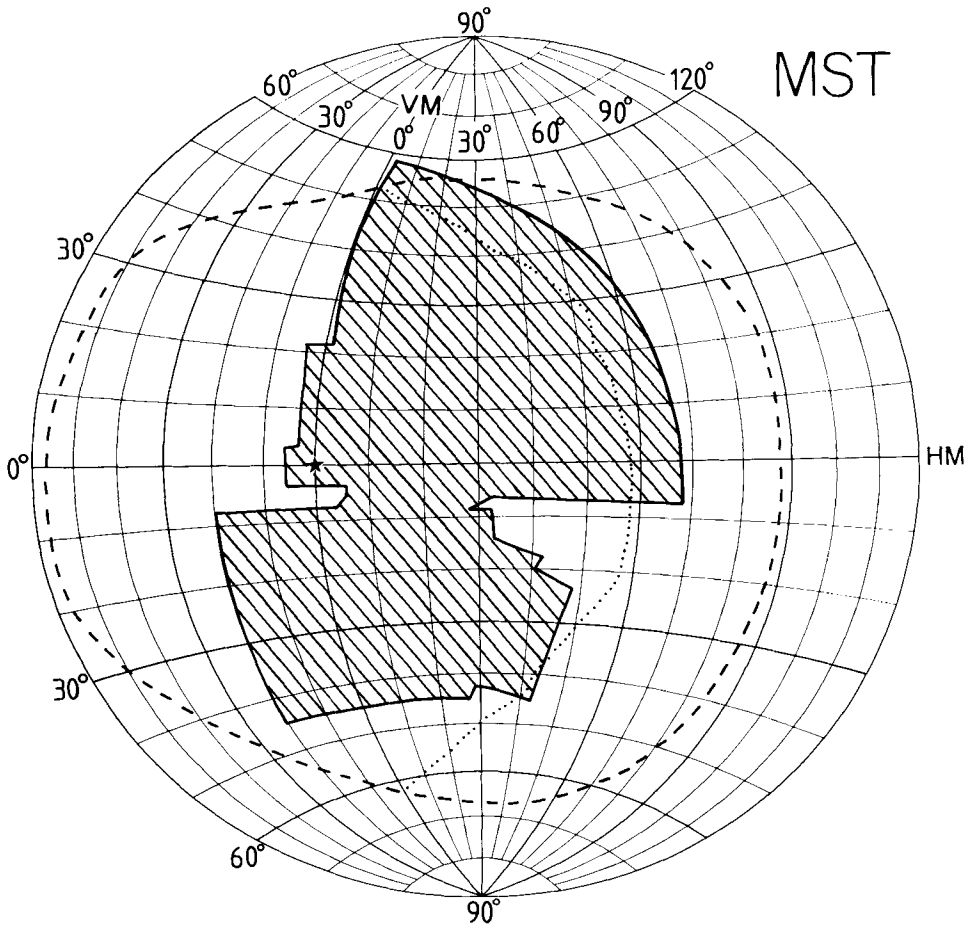

Fig. 18. Extent of the visual field represented in MST (shaded). See also legend to Figure 7.

nels in V1 is still unsettled. If one takes into account the hypothesis of Schein and de Monasterio ('87), the lower variation in MT could reflect its dominance by a single channel, the magnocellular one (Felleman and Van Essen, '87).

Comparisons between MT and V1

The observation of similar slopes and different intercepts when comparing M functions of MT and V1 in most animals suggests that the visual map of MT is, fundamentally, a compression of the map found in V1 (Gattass and Gross, '81). However, there are important ways in which the visuotopic maps of these areas differ. As suggested by Gattass and Gross ('81), some of the differences can be accounted for by the large receptive fields found in MT. For example, while in V1 there are receptive field centers close to the VM throughout its extent, in MT receptive field centers falling at the VM are restricted to the central 15° (see Fig. 6). Beyond this point, with increasing eccentricity, receptive field centers corresponding to sites located at the border of MT are progressively distant from the VM, although these receptive fields include parts of this meridian. Therefore, a different criterion must be used to define the vertical meridian representation in MT, as compared with V1 and V2. Also, inasmuch as receptive fields have finite sizes and the invasion into the ipsilateral visual field is small, no receptive field centers were found at the center of gaze. Other differences between MT and V1 arise from the greater scatter in the former. For example, in our study, iso-eccentricity lines were drawn based on receptive field centers only. Thus, the visual maps of MT (Fig. 8) do not take into account the scatter and receptive field size (see Fig. 13) and are somewhat more "schematic" than those proposed for V1.

The visual maps of MT and V1 also differ with respect to the relative emphasis in foveal representation. Very few receptive fields were recorded at the foveal representation of MT in all animals, and this small sample did not allow us to estimate the variation of foveal M in MT. However, measurements on flattened maps revealed that the foveal representation occupies about 9% of the total surface area of MT. In comparison, the ratio between the representations of the fovea and of the binocular field in V1 is about 15%. Moreover, the functions relating M with eccentricity calculated along isopolar and isoeccentric dimensions in MT were similar, while V1 and V2 present a greater polar magnification (Gattass et al., '87; Rosa et al., '88b).

Area MT: comparisons with other primate species

The diurnal New World monkey *Cebus* is more comparable in size and sulcal pattern to the diurnal Old World monkey *Macaca* than to the nocturnal New World monkey

Aotus, with whom the *Cebus* shares a more recent common ancestor. Studies of the visuotopic organization of V1 (Gattass et al., '87) and of V2 (Rosa et al., '88b) showed that these areas in the *Cebus* do not differ from those of Old World monkeys in size, location, and visuotopic organization; they, however, differ from those of *Aotus* (Allman and Kaas, '71b, '74a). The terminology used in these species is somewhat different, but the organization of the visual areas in dorsal superior temporal sulcus in *Macaca* and in *Cebus* and in the caudal medial temporal gyrus in *Aotus* presents a number of similarities, which suggest the existence of homologies.

Although some dispute still exists on the definition of the borders of MT, the homology of MT of the macaque with that of the New World monkeys is now well founded (Maunsell and Van Essen, '83a,b; Desimone and Ungerleider, '86). The central field representation of MT is more heavily myelinated than the far peripheral representation in both *Macaca* and *Aotus* (Allman and Kaas, '71a; Gattass and Gross, '81; Desimone and Ungerleider, '86), a result which lends generality to our conclusions regarding the myeloarchitectonic extent of MT in *Cebus*.

The use of different criteria to define the borders of area MT is, at least in part, responsible for the apparently conflicting results of previous studies (Allman and Kaas, '71a; Gattass and Gross, '81; Van Essen et al., '81; Desimone and Ungerleider, '86; Maunsell and Van Essen, '87; Komatsu and Wurtz, '88). For example, Van Essen et al. ('81) and Maunsell and Van Essen ('87) found a clear correspondence between the lateral border of MT determined both by myeloarchitectonic and directional selectivity criteria. In addition, they concluded that this border would not always correspond to the representation of the lower vertical meridian and that MT would include rerepresentations of the lower quadrant (Maunsell and Van Essen, '87). However, in another study in the macaque (Erickson, '86), direction selectivity was observed both in MT and in an adjacent dorsal zone which shows a distinct architectonic pattern. In this study, dorsal to MT we also observed an area with a distinct myeloarchitectonic pattern (DZ) in a region corresponding to the dorsally located zone described by Erickson ('86); we distinguished this region from MT in order to avoid a double representation of the lower visual quadrant. Furthermore, although our study was based on multiunit recordings and we did not study neuronal properties systematically, we have observed direction selectivity in several recording sites located in DZ, as did Erickson ('86) based on a single-unit study in the macaque. The difference in criteria to define the borders of MT could explain the existence of the inferior oblique bias reported by Maunsell and Van Essen ('87) in MT of the macaque. These authors might have included part of DZ, an area which contains a representation of the lower visual quadrant, in MT. They had suggested that this bias could be related to the highly developed manipulative behavior of this monkey. However, in the *Cebus*, the representation of the visual field in MT is highly variable and does not present such a bias, in spite of the fact that this animal displays the best performance in object manipulation among monkeys. They are, in fact, superior to macaques in this aspect (Torigoe, '86). Therefore, the amount of representational bias in MT does not seem to be correlated with the degree of manipulative capability of the genera. Thus, our definition of MT better conforms with the original of Allman and Kaas ('71a) for New World monkeys. Taking into consideration the different definitions of the borders of MT, the similarities in the visuotopic organization of MT between *Cebus* and *Macaca* become clear. The differences in the visual topography of MT observed between *Cebus* and *Macaca* are comparable to the individual variability observed among animals of each genus (Gattass and Gross, '81; Van Essen et al., '81; Desimone and Ungerleider, '86; Maunsell and Van Essen, '87). In the *Cebus* the amount of individual variability in MT seems to be larger than that observed for V1 and V2 (Gattass et al., '87; Rosa et al., '88b; unpublished data).

The size of MT in the *Cebus* is similar to that of similar-sized macaques. Furthermore, the size of MT relative to V1 is also similar in *Cebus*, *Macaca*, and *Aotus*. This result contrasts with the size of V2 relative to V1, which is much smaller in *Aotus* than in other species (Rosa et al., '88b). These facts could be related to the different roles of these areas in the visual processing of form and motion under scotopic vs. photopic conditions.

The visual maps of MT in *Aotus* and in the prosimian *Galago* present a smaller emphasis on the representation of the fovea than do those of both *Cebus* and *Macaca*. While in the *Cebus* the 10° iso-eccentricity line is located roughly in the middle of area MT, in *Aotus* and *Galago* this location corresponds to the 30° isoeccentricity line (Allman and Kaas, '71a; Allman et al., '73). In order to compare the visual topography in MT, we have used our automatic system to calculate M functions for the owl monkey, based on data from Allman and Kaas ('71a—Fig. 9, '74b—Fig. 2), in the range of 5 to 50°, and for *M. fascicularis*, based on data from Gattass and Gross ('81—Fig. 4) and from Maunsell and Van Essen ('87—Fig. 3), in the range of 0.2 to 50°. The slopes and intercepts of M functions for MT in *Aotus*, *Macaca*, and *Cebus* are not statistically different. The differences in the size of MT between these species must, then, arise from a compression of the most central (below 5°) representation in *Aotus*.

We have also compared the scatter in receptive field position of MT in *Cebus*, *Macaca*, and *Aotus* as calculated with the same methods. While scatter in receptive field positions in *Cebus* and *Macaca* is similar and increases with increasing eccentricity, in *Aotus* it is fairly constant. The symmetry in the extent of representation of the upper and lower visual quadrants and the existence of a representation of the entire field of vision are also characteristics of area MT in *Aotus* and in the *Galago*, nocturnal primates, but are not always present in *Cebus* monkeys and in macaques (Allman and Kaas, '71a; Allman et al., '73; Gattass and Gross, '81; Desimone and Ungerleider, '86; Maunsell and Van Essen, '87).

Visual areas surrounding MT

While the homology of MT in New and Old World monkeys can now be considered as established, the correspondence of DZ to previously described visual areas is less clear. V4T is a myeloarchitectonically distinct zone, in the macaque confined to ST, which commonly borders the full length of MT dorsolaterally (Desimone and Ungerleider, '86; Gattass et al., '88). In sections stained for myelin V4T contains a distinctive light myelination in all cortical layers (Ungerleider and Desimone, '86). In V4T, there was a tendency for receptive fields corresponding to sites located at the V4T/MT border to lie close to the vertical meridian and for those at the V4T/V4 border to lie close to the horizontal meridian (Desimone and Ungerleider, '86; Gattass et al., '88).

Due to the coarseness of the visual topography, V4T was primarily defined in the macaque based on myeloarchitectonic criteria. In the *Cebus* we defined DZ primarily on the basis of visual topography and then defined its anatomical correlates. The different descriptions of the myeloarchitectonic characteristics of these regions in the *Cebus* and in the macaque impose the use of different names, although both zones have a crude mirror-image representation of at least the central portion of the inferior quadrant of MT (Desimone and Ungerleider, '86; Gattass et al., '88).

In *Aotus,* Sereno et al. ('87) restudied the dorsolateral crescent (DL) and found three representations of the lower visual quadrant in the dorsal half of this region. The most anterior of these areas, DL proper, seems to correspond to DZ of the present study and to V4T of the macaque. Like V4T in the macaque (Desimone and Ungerleider, '86; Gattass et al., '88) and DL proper in *Aotus* (Sereno et al., '87), in the *Cebus* we found no systematic representation of the upper visual field in area DZ or in an area contiguous to the foveal representation of DZ bordering area MT ventrally. In addition, while fluorescent tracers injected in the region of representation of the lower quadrant in V1 showed label dorsal to MT, no corresponding label was found after upper quadrant injections (Piñon et al., '86; Sousa et al., '87).

MST and FST in the *Cebus* were defined based on the transitions of the myeloarchitectonic patterns of receptive field sequences and sizes at their borders with MT. MST is located anterior to MT, similarly to MST in the macaque (Desimone and Ungerleider, '86) and to area ST in the *Aotus* (Weller et al., '84; Cusick et al., '84). Recently, Komatsu and Wurtz ('88) suggested that part of FST as defined by Desimone and Ungerleider ('86) is in fact the foveal representation of the lateral subdivision of MST, named MSTL. Our data do not allow us to rule out this possibility, inasmuch as we agree that a single functional area may be myeloarchitectonically heterogeneous and that most receptive fields recorded close to the MT/FST border are central (see Fig. 15). Komatsu and Wurtz ('88), however, found that dorsal MST is a well-defined area as regards receptive field properties while MSTL shows more heterogeneous unit properties. Therefore, we think this issue deserves more study, and we prefer to name this region FST in the *Cebus,* following the same criteria used by Desimone and Ungerleider ('86) in the macaque.

In summary, visual area MT and neighboring areas in the *Cebus* are similar to those found in the macaque. In MT, the differences related to the emphasis in central vision, to the extent of the visual field representation, and to the scatter observed when comparing these species with *Aotus* cannot, thus, be considered as general differences between Platyrrhini and Catarrhini; more likely they are related to differences in the visual behavior of nocturnal vs. diurnal primates. This hypothesis is supported by the observation that, in all of these aspects, *Aotus* is more similar to the nocturnal lorisiform prosimian *Galago* than to other simians.

ACKNOWLEDGMENTS

The authors are grateful to Dr. C.E. Rocha-Miranda for helpful comments on the manuscript. Thanks are due to Edil Saturato da Silva Filho and Edna M.L. da Silva for technical assistance, to Virginia P.G.P. da Rosa for the illustrations, and to Sandra B. da Rocha, Alba Valéria Peres, and Ma. Fernanda M. Lamego for typing the manuscript. We gratefully acknowledge Fundação Parque Zoológico de São Paulo for the donation of the animals used in this study. This research was supported by grants from CNPq (30.0188/80, 30.5654/76, 40.6434/87.5, 40.8179-88), FINEP (42.0375.00), and CEPG/UFRJ to the authors.

LITERATURE CITED

Albright, T.D., and R. Desimone (1987) Local precision of visuotopic organization in the middle temporal area (MT) of the macaque. Exp. Brain Res. *65*:582–592.

Allman, J.M., and J.H. Kaas (1971a) A representation of the visual field in the caudal third of the middle temporal gyrus of the owl monkey (*Aotus trivirgatus*). Brain Res. *31*:85–105.

Allman, J.M., and J.H. Kaas (1971b) Representation of the visual field in striate and adjoining cortex of the owl monkey (*Aotus trivirgatus*). Brain Res. *39*:89–106.

Allman, J.M., and J.H. Kaas (1974a) The organization of the second visual area (V-II) in the owl monkey: A second-order transformation of the visual hemifield. Brain Res. *76*:247–265.

Allman, J.M., and J.H. Kaas (1974b) A crescent-shaped cortical visual area surrounding the middle temporal area (MT) in the owl monkey (*Aotus trivirgatus*). Brain Res. *81*:199–213.

Allman, J.M., J.H. Kaas, and R.H. Lane (1973) The middle temporal visual area (MT) in the bushbaby, *Galago senegalensis*. Brain Res. *57*:197–202.

Cusick, C.G., H.J. Gould III, and J.H. Kaas (1984) Interhemispheric connections of visual cortex of owl monkeys (*Aotus trivirgatus*), marmosets (*Callithrix jacchus*), and galagos (*Galago crassicaudatus*). J. Comp. Neurol. *230*:311–336.

Daniel, P.M., and D. Whitteridge (1961) The representation of the visual field on the cerebral cortex in monkeys. J. Physiol. (Lond.) *159*:203–221.

Desimone, R., and L.G. Ungerleider (1986) Multiple visual areas in the caudal superior temporal sulcus of the macaque. J. Comp. Neurol. *246*:164–189.

Dow, B.W., R.G. Snyder, R.G. Vautin, and R. Bauer (1981) Magnification factor and receptive field size in foveal striate cortex of the monkey. Exp. Brain Res. *44*:213–228.

Dubner, R., and S.M. Zeki (1971) Response properties and receptive fields of cells in an anatomically defined region of the superior temporal sulcus of the monkey. Brain Res. *35*:528–532.

Erickson, R.G. (1986) Representation of the Fovea and Identification of the Foveal Tracking Cells in the Superior Temporal Sulcus of the Macaque Monkey. PhD thesis, State University of New York, Buffalo, N.Y., 141 pp.

Felleman, D.J., and D.C. Van Essen (1987) Receptive field properties of neurons in area V3 of macaque monkey extrastriate cortex. J. Neurophysiol. *57*:889–920.

Fiorani, M., Jr., R. Gattass, M.G.P. Rosa, and A.P.B. Sousa (1985) Visual topography of MT in the *Cebus* monkey. Braz. J. Med. Biol. Res. *18*(5–6):638 (Abstract).

Fleagle, J.E., T.M. Bown, J.D. Obradovich, and E.L. Simons (1986) Age of the earliest African anthropoids. Science *234*:1247–1249.

Freese, C.H., and J.R. Oppenheimer (1981) The capuchin monkeys, genus *Cebus*. In A.F. Coimbra-Filho and R.A. Mittermeier (eds): Ecology and Behaviour of Neotropical Primates, Vol. I. Rio de Janeiro: Academia Brasileira de Ciências, pp. 331–390.

Gattass, R., and C.G. Gross (1981) Visual topography of the striate projection zone in the posterior superior temporal sulcus (MT) of the macaque. J. Neurophysiol. *46*:621–638.

Gattass, R., M. Fiorani, Jr., M.G.P. Rosa, and A.P.B. Sousa (1986a) Visual areas in the posterior superior temporal sulcus in the *Cebus*. Proc. Soc. Neurosci. *12*:1366 (Abstract).

Gattass, R., A.P.B. Sousa, and E. Covey (1986b) Cortical visual areas of the macaque: Possible substrates for pattern recognition mechanisms. Exp. Brain Res. [Suppl.] *11*:1–20.

Gattass, R., A.P.B. Sousa, and M.G.P. Rosa (1987) Visual topography of V1 in the *Cebus* monkey. J. Comp. Neurol. *259*:529–548.

Gattass, R., A.P.B. Sousa, and C.G. Gross (1988) Visuotopic organization and extent of V3 and V4 in the macaque. J. Neurosci. *8*:1831–1845.

Hoffstetter, R. (1974) Phylogeny and geographical deployment of the primates. J. Hum. Evol. *3*:327–350.

Hubel, D.H., and T.N. Wiesel (1974) Uniformity of monkey striate cortex: A parallel relationship between field size, scatter, and magnification factor. J. Comp. Neurol. *158*:295–306.

Komatsu, H., and R.H. Wurtz (1988) Relation of cortical areas MT and MST to pursuit eye movements. I. Localization and visual properties of neurons. J. Neurophysiol. *60*:580–603.

Lin, C.S., R.E. Weller, and J.H. Kaas (1982) Cortical connections of striate cortex in the owl monkey. J. Comp. Neurol. *211*:165–176.

Livingstone, M.S., and D.H. Hubel (1988) Do the relative mapping densities of the magno- and parvocellular systems vary with eccentricity? J. Neurosci. *8*:4334–4339.

Lund, J.S., R.D. Lund, A.E. Hendrickson, A.H. Bunt, and A.F. Fuchisi (1975) The origin of efferent pathways from the primary visual cortex, area 17, of the macaque monkey as shown by retrograde transport of horseradish peroxidase. J. Comp. Neurol. *164*:287–305.

Mac Fadden, B.J. (1987) Chronology of tertiary primate localities in South America, with emphasis on the earliest-known (25 MYR) occurrence. Int. J. Primatol. *8*(Suppl. 5):15 (Abstract).

Maunsell, J.H.R., J.L. Bixby, and D.C. Van Essen (1979) The middle temporal area (MT) in the macaque: Architecture, functional properties and topographic organization. Proc. Soc. Neurosci. *5*:796 (Abstract).

Maunsell, J.H.R., and D.C. Van Essen (1983a) Functional properties of neurons in middle temporal visual area of the macaque monkey. I. Selectivity for stimulus direction, speed and orientation. J. Neurophysiol. *49*:1127–1147.

Maunsell, J.H.R., and D.C. Van Essen (1983b) Functional properties of neurons in middle temporal visual area of the macaque monkey. II. Binocular interactions and sensitivity to binocular disparity. J. Neurophysiol. *49*:1148–1167.

Maunsell, J.H.R., and D.C. Van Essen (1983c) The connections of the middle temporal visual area (MT) and their relationship to a cortical hierarchy in the macaque monkey. J. Neurosci. *3*:2563–2586.

Maunsell, J.H.R., and D.C. Van Essen (1987) Topographic organization of the middle temporal visual area in the macaque monkey: Representational biases and the relationship to callosal connections and myeloarchitectonic boundaries. J. Comp. Neurol. *266*:535–555.

McIllwain, J.L. (1976) Large receptive fields and spatial transformations in the visual system. Int. Rev. Physiol. *10*:223–249.

Montero, V.M. (1980) Patterns of connections from the striate cortex to cortical visual areas in superior temporal sulcus of macaque and middle temporal gyrus of owl monkey. J. Comp. Neurol. *189*:45–55.

Piñon, M.C., A.P.B. Sousa, M.G.P. Rosa, and R. Gattass (1986) Aferentes corticais da área visual primária (V1) do macaco *Cebus*. Proc. Soc. Braz. Neurosci. *1*:77 (Abstract).

Rockland, K.S., and D.N. Pandya (1981) Cortical connections of the occipital lobe in the rhesus monkey: Interconnections between areas 17, 18, 19 and the superior temporal sulcus. Brain Res. *212*:249–270.

Rosa, M.G.P., R. Gattass, and M. Fiorani, Jr. (1988a) Complete pattern of ocular dominance stripes in V1 of a New World monkey, *Cebus apella*. Exp. Brain Res. *72*:645–648.

Rosa, M.G.P., A.P.B. Sousa, and R. Gattass (1988b) Representation of the visual field in the second visual area in the *Cebus* monkey. J. Comp. Neurol. *275*:326–345.

Sanides, F. (1972) Representation in the cerebral cortex and its areal lamination patterns. In G.H. Bourne (ed): The Structure and Function of the Nervous Tissue. New York: Academic Press, pp. 329–453.

Schein, S.J., and F.M. de Monasterio (1987) The mapping of retinal and geniculate neurons onto striate cortex of macaque. J. Neurosci. *7*:996–1009.

Schwartz, E.L. (1980) Computational anatomy and functional architecture of striate cortex: A spatial mapping approach to perceptual coding. Vision Res. *20*:645–669.

Sereno, M.I., C.T. McDonald, and J.M. Allman (1987) Multiple visual areas between V2 and MT in the owl monkey. Proc. Soc. Neurosci. *13*:625 (Abstract).

Sousa, A.P.B., R. Gattass, M.C. Piñon, and M.G.P. Rosa (1987) Cortical afferents to area V1 in the *Cebus* monkey. Proc. Soc. Neurosci. *13*:625 (Abstract).

Spatz, W.B., and J. Tigges (1972) Experimental-anatomical studies on the "middle temporal visual area (MT)" in primates. I. Efferent cortico-cortical connections in the marmoset *Callithrix jacchus*. J. Comp. Neurol. *146*:451–464.

Talbot, S.A., and W.H. Marshall (1941) Physiological studies on neural mechanisms of visual localization and discrimination. Am. J. Ophthalmol. *24*:1255–1264.

Torigoe, T. (1986) Object manipulation in primates: A comparative psychological approach to human behaviour. Hiroshima Forum Psychol. *11*:89–99.

Ungerleider, L.G., and M. Mishkin (1979) The striate projection zone in the superior temporal sulcus of *Macaca mulatta*: Location and topographic organization. J. Comp. Neurol. *188*:347–366.

Ungerleider, L.G., and R. Desimone (1986a) Projections to the superior temporal sulcus from the central and peripheral field representations of V1 and V2. J. Comp. Neurol. *248*:147–163.

Ungerleider, L.G., and R. Desimone (1986b) Connections of visual area MT in the macaque. J. Comp. Neurol. *248*:190–222.

Van Essen, D.C., J.H.E. Maunsell, and J.L. Bixby (1981) The middle temporal visual area in the macaque: Myeloarchitecture, connections, functional properties, and topographical organization. J. Comp. Neurol. *199*:293–326, 1981.

Van Essen, D.C., W.T. Newsome, and J.H.R. Maunsell (1984) The visual field representation in striate cortex of the macaque monkey: Asymmetries, anisotropies and individual variability. Vision Res. *24*:429–448.

Van Essen, D.C., W.T. Newsome, J.H.R. Maunsell, and J.L. Bixby (1986) The projections from striate cortex (V1) to areas V2 and V3 in the macaque monkey: Asymmetries, areal boundaries and patchy connections. J. Comp. Neurol. *244*:451–480.

Weller, R.E., and J.H. Kaas (1983) Retinotopic patterns of connections of area 17 with visual areas V-II and MT in macaque monkeys. J. Comp. Neurol. *220*:253–279.

Weller, R.E., J.T. Wall, and J.H. Kaas (1984) Cortical connections of the middle temporal visual area (MT) and the superior temporal cortex in owl monkeys. J. Comp. Neurol. *228*:81–104.

Zeki, S.M. (1971) Convergent input from the striate cortex (area 17) to the cortex of the superior temporal sulcus in the rhesus monkey. Brain Res. *28*:338–340.

Zeki, S.M. (1974) Functional organization of a visual area in the posterior bank of the superior temporal sulcus of the rhesus monkey. J. Physiol. (Lond.) *236*:549–573.

Zeki, S.M. (1978) Uniformity and diversity of structure and function in rhesus monkey prestriate visual cortex. J. Physiol. (Lond.) *277*:273–290.

Zeki, S.M. (1980) The response properties of cells in the middle temporal area (area MT) of owl monkey visual cortex. Proc. R. Soc. Lond. [Biol.] *207*:239–248.